

[Open Peer Review on Qeios](#)

# Investigations on Input Impedance and Radiation Pattern of a UWB Antenna for Microwave Imaging

Olayiwola Charles Adesoba<sup>1</sup>, Richard Olalekan Taiwo<sup>2</sup>

<sup>1</sup> Federal University of Technology, Akure

<sup>2</sup> Ekiti State University

**Funding:** No specific funding was received for this work.

**Potential competing interests:** No potential competing interests to declare.

## Abstract

Investigations carried out on the Input Impedance and Radiation Pattern of an Ultra-wideband (UWB) antenna are presented in this study. The proposed antenna is fabricated on an FR4 printed circuit board with a rectangular aperture. Major applications of UWB technology are presented. The fundamental characteristics of the antenna, such as input impedance, return loss, radiation pattern, and realized gain, are obtained. Investigations on how to improve the directivity of the proposed antenna are also presented in this study. The antenna demonstrates good impedance bandwidth ( $S_{11} \leq -10\text{dB}$ ) from about 4GHz to 10.6GHz, except in the case when the width  $W$  of the T-shaped stub was varied. A commercial simulation tool – CST Microwave Studio – is used for the optimization of the proposed antenna. The proposed antenna operates almost over the entire UWB band (3.1-10.6GHz), except at lower frequencies of 3.1-4GHz. The response of the designed UWB signal starts at 3.1-10.6GHz, giving a good performance between 4GHz to 10.6GHz with an operational bandwidth of 6.6GHz. The input impedance is well matched, as a return loss of 10dB is obtained between 4-10.6GHz. The return loss decreases even more at 4-5GHz and at 8-10GHz, which means that the proposed UWB antenna transmits a high percentage of its power while a very low power is reflected back.

Olayiwola Charles Adesoba<sup>1,\*</sup>, and Richard Olalekan Taiwo<sup>2</sup>

<sup>1</sup> Department of Computer Engineering, Federal University of Technology Akure, Akure, 340110, Ondo, Nigeria.

<sup>2</sup> Department of Computer Science, Ekiti State University, Ado-Ekiti, 362103, Ekiti, Nigeria.

\*Corresponding author. E-mail: [ocadesoba@futa.edu.ng](mailto:ocadesoba@futa.edu.ng)

**Keywords:** Ultra-wideband (UWB), Return loss, Radiation pattern, Impedance bandwidth, Frequency Selective Surface (FSS).

## 1. Introduction

UWB technology can be used practically in all cases where a highly precise remote observation of objects at short distances and their motion is required. UWB radars can be used in automobile traffic control systems to prevent collisions while driving and parking; they can also be used in security systems as signaling sensors which provide detection of unaccepted intrusion into the protected area [1]. They are also useful in hospitals and homes where they can provide remote measuring of the heart and respiratory systems. UWB radars are also used for the monitoring of liquid levels in a confined container. UWB technology has yielded some more interest in the daily applications at present. The first ideas of commercial applications focused on High Data Rate applications such as multimedia communications or wireless USB, thanks to the channel capacity of UWB following the Shannon-Hartley formula which is expressed as;

$$C = B \cdot \log_2 \left( 1 + \frac{S}{N} \right)$$

Where C is the channel capacity in bits/sec, B is the channel bandwidth in Hertz, S is the received signal power in Watts, and N is the noise power in Watts [2]. Major applications of UWB technology are explained in the sub-sections below:

### Communication Systems

UWB technology is one of the foreseen applications for short-range indoor communication, and a lot of consideration has been given to it in recent times. To reduce interference with existing narrowband technology, UWB systems expand the transmitted power over an immensely large frequency band up to 10.6GHz, and the power spectral density of the signal is very low [3]. The solution on the market for today's indoor applications is ultrasonic and infrared approaches. The line-of-sight propagation in infrared technology cannot be guaranteed all the time [4]. It is also affected by shadows and light-related interferences. The ultrasonic approach propagates with confined penetration. Shadows do not really affect UWB technology, and transmission through objects is possible. The innovative communication method of UWB at a low data rate gives numerous benefits to the government and private sectors. For instance, the wireless connection of computer

peripherals such as keyboard, monitor, mouse, joystick, and printer can utilize UWB technology. It allows the operation of multiple devices without interference at the same time in the same space. It can also be used as a communication link in a sensor network.

## Positioning/Localisation Systems

Positioning system is a method that defines the coordinates of a radiating object based on a distinction at the moment of the signal appearance (a time delay distinction) to several receivers located in the area [1]; it is made known that a time digitizer converter (TDC) is used to define a distinction of delay times of signals in each of the received signals of the system. The use of a time digitizer converter (TDC) is to measure the time between a pulse switching on and coming off one or more pulses switching off with high accuracy. The system begins with simultaneous switching on of the time digitizer converters (TDC) of all received channels by the general pulse switching on; meanwhile, the signals of the object accepted by receivers are the pulses switching off. The time intervals received on all received channels are transferred to the device for information processing, where the definition of the belonging of the accepted time intervals to the same signal of the object (primary processing) and the calculation of the coordinates of the object, with a display of the position of the object on a personal computer (secondary processing), is performed in the field [1].

## Bio-imaging Systems

Due to the high resolution and great penetration of UWB radar, it gives us assurance for the great use in the bio-medical field, such as cancer detection, which is the concentration of this project. The use of UWB is needed in the bio-medical field to reduce the rate of fatality due to malignant tumors affecting our women. The most commonly used for the diagnosis of malignant tumors are Magnetic Resonance Imaging, Computed Tomography, and Ultrasound. The Magnetic Resonance Imaging and Computed Tomography techniques are very useful for cancer diagnosis, but they are not often used as they are very expensive.

In a study by [5], tumors larger than 1-2cm in size can be detected by both Computed Tomography and Ultrasound imaging techniques with a false rate of 50% and detection rates of 72%. On similar-sized tumors, the Magnetic Resonance Imaging method yields false alarm and detection rates of 27% and 77%, respectively. It can be deduced from this study that the use of the Magnetic Resonance Imaging technique is more reliable compared to Ultrasound and Computed Tomography, but its limitation is that it is expensive. UWB imaging systems have shown promising results in the detection of tumors for early breast cancer detection [6]. The elementary property on which UWB imaging relies is the large difference between malignant tissue and normal tissue [7]; [6]. In UWB imaging systems, a wideband pulse is transmitted from an antenna to the body and allowed to impact, and as the pulse propagates through the various tissues of the body, reflection occurs at interfaces between the different tissues of the body. This backscattered signal can be used to map different layers of the body using methods similar to Ultrasound Imaging [5]. The difference between malignant and normal tissue has been estimated to be on the order of a 2 to 1 ratio for breast cancer [7].

## 2. Related Works

The major challenge of the design of a compact coplanar waveguide-fed ultra-wideband monopole-like slot antenna, earlier reviewed by [8], was the emission of energy as a result of back radiation, which made it not completely unidirectional. This is the more reason why the author wouldn't agree with this design, and the author thought there should be possible ways of reducing the back radiation and a way to further improve the impedance matching of the antenna, which made the author further his research on how to achieve unidirectional radiation over an ultra-wideband frequency range and a way to improve the impedance bandwidth and reduce the back radiation. Fortunately, the authors were able to see a conference publication, also by Qing and Chen, presented in 2011, whereby efforts had been made to improve all the limitations they had in their previous paper in 2009. This paper, presented in 2011 by [9], seems to be a bit related to this study; so, therefore, a more detailed review would be given on how they went about solving the challenges they encountered in their earlier design. The antenna was designed so as to cover both low and high-frequency bands. This antenna was designed and compared to both reference antennas 1 and 2. When compared with the coplanar waveguide-fed UWB slot antenna, the slot ground and feed line are moved from the top layer to the bottom layer, and the feed line has been changed to a fork-shaped tuning stub. This antenna, designed by Zhu et al. (2011), can also be seen as the composition of a UWB slot antenna excited by a fork-shaped tuning stub, which is the reference antenna 2, on the bottom layer, and a circular patch on the top layer, respectively<sup>[10]</sup>. It was ensured that the reflector's dimension is the same for the three types of UWB antennas, and the dimension of the radiator is the same as the coplanar waveguide-fed UWB slot antenna.

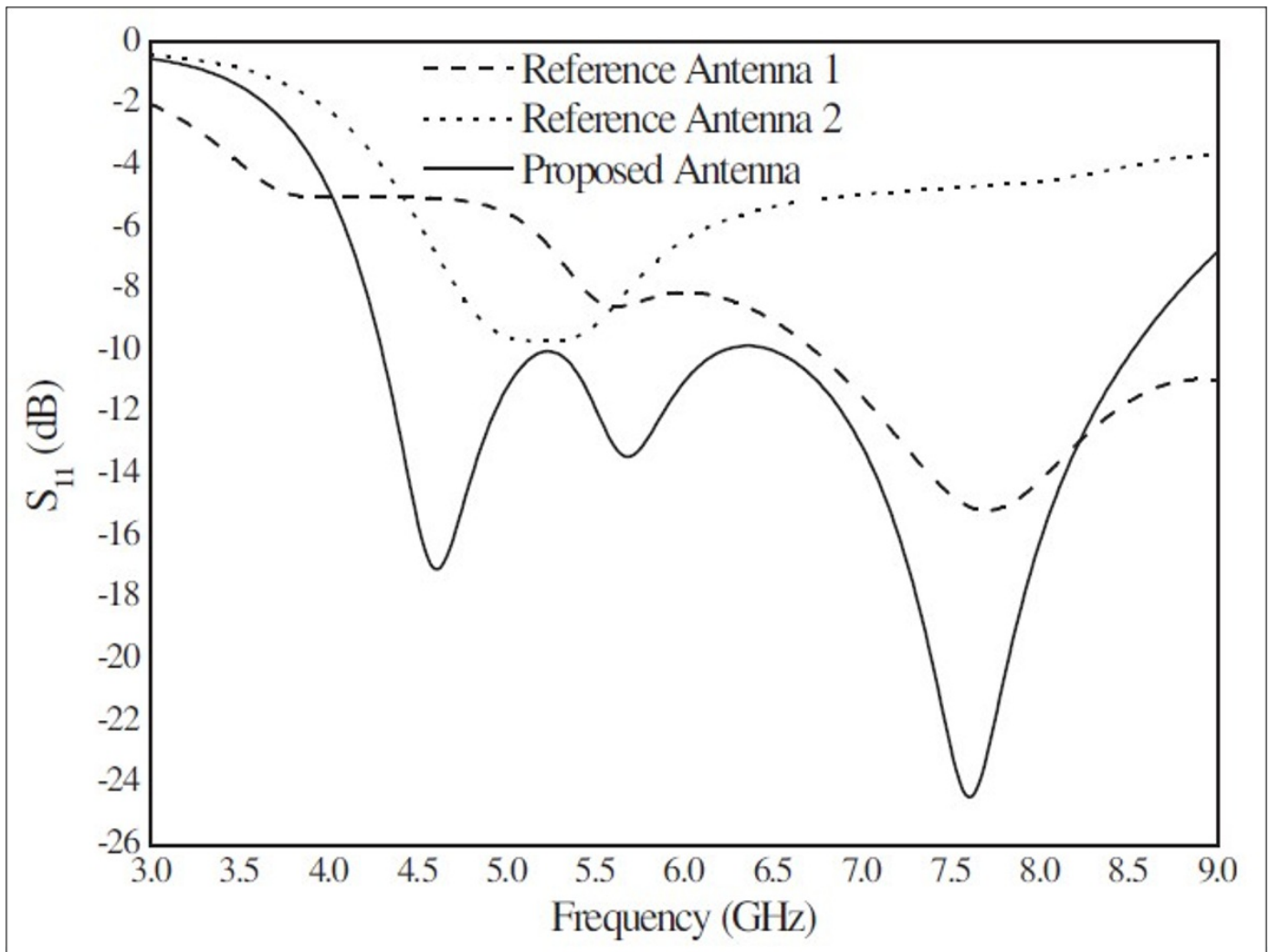


Fig. 1. Simulated Reflection Coefficients among the Three Types of Antenna [11]

The simulated reflection coefficient among the three types of antennas, as seen in Figure 1, shows that the proposed directional antenna has better impedance matching at the low-frequency band when compared with the CPW-fed UWB slot antenna (reference antenna 1), because of the separation of the slot ground plane on the bottom layer from the circular patch on the top layer, and is also seen to be improved at a high-frequency band because of the circular patch added when compared with the fork-shaped excited UWB slot antenna (reference antenna 2) [10]. In terms of antenna gain, the proposed directional antenna exhibits the same variation trend as the fork-shaped excited UWB slot antenna over the whole frequency band. It has a higher gain than the fork-shaped excited UWB slot antenna because of the circular patch radiation. When compared with the CPW-fed UWB slot antenna, the gain greatly improved from about 4GHz to 6GHz due to good impedance matching.

Most of the UWB antennas presented so far exhibit radiation patterns similar to those of acceptable monopole/dipole antennas [12][13][14]. It is suspected that the antenna efficiencies will be degraded owing to omni-directional/bi-directional radiation when they are attached to walls, metallic objects, or the human body. To avoid the degradation of antenna efficiencies, a directional UWB antenna should be utilized, which brought about the high desire for the development of a UWB antenna having directional radiation characteristics [8].

## Effect of a Metallic Cavity on a Slot Antenna

To achieve unidirectional radiation over an ultra-wideband frequency range, the addition of an open metallic cavity underneath a monopole-like slot antenna is required. In the design of a miniaturized directional UWB antenna presented by [9], Styrofoam was used as the conducting supporting material, with an open cavity placed underneath a monopole-like slot antenna, which produced fascinating impedance matching and allowed the antenna to produce unidirectional radiation over an ultra-wideband frequency range. The cavity contains a microwave absorber used to further improve the impedance bandwidth and reduce the back emission of energy, known as back radiation.

The 3-dimensional view and the cross-sectional view of the proposed miniaturized UWB antenna are shown in Figure 2 and Figure 3 respectively.

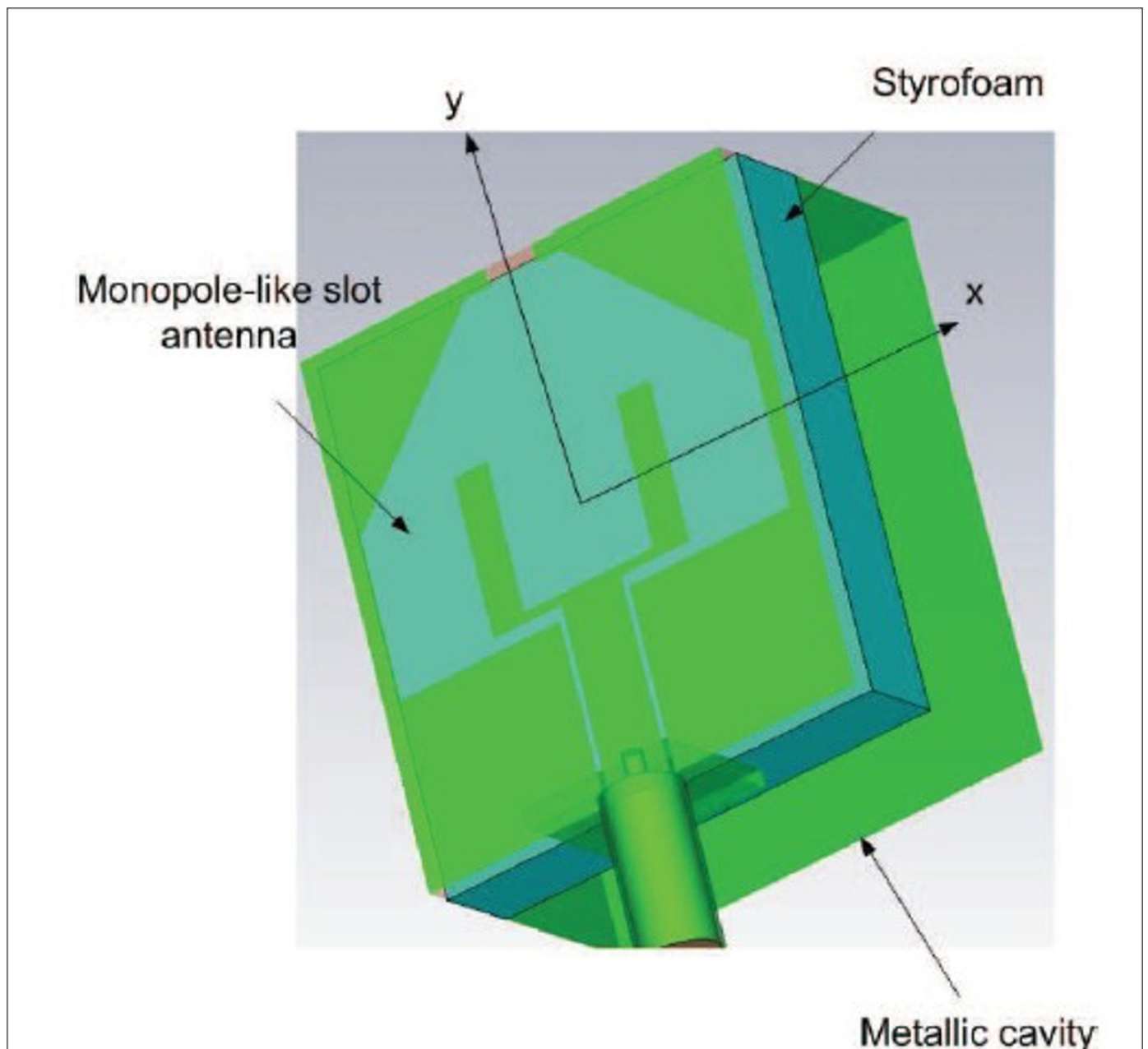
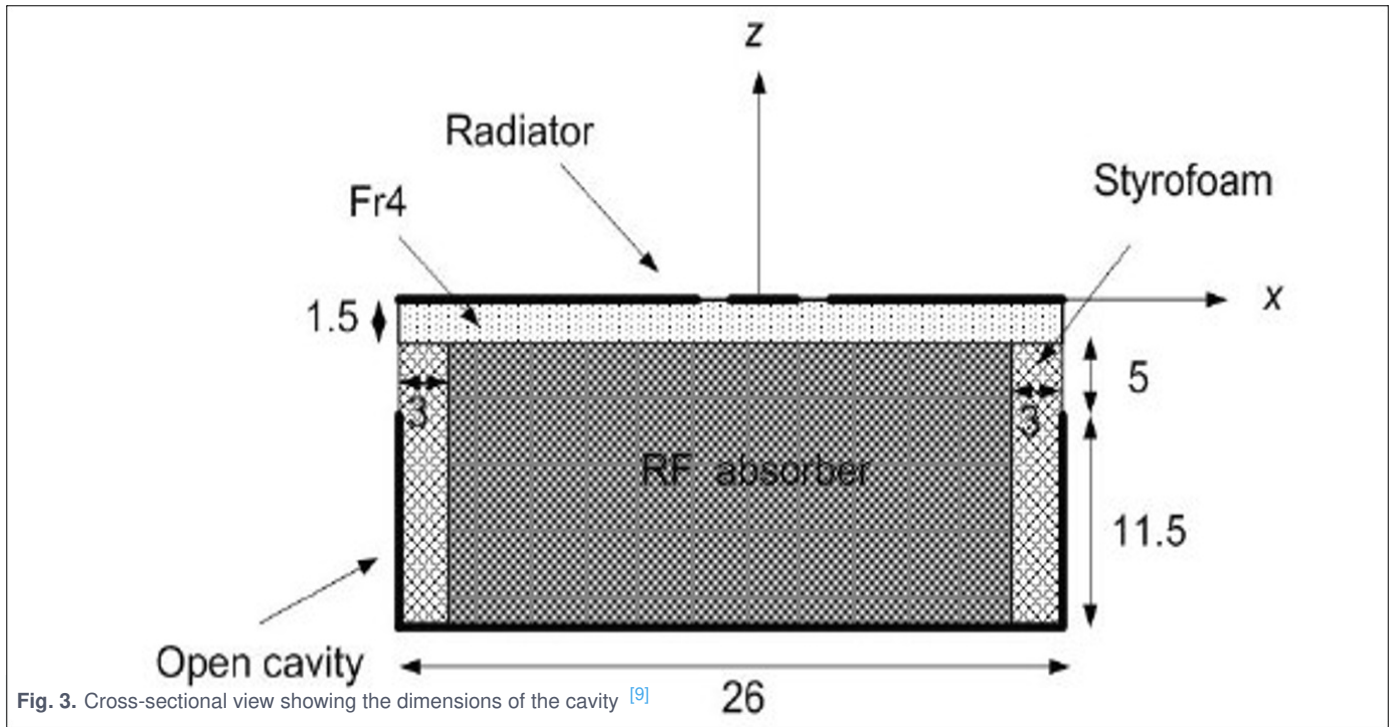


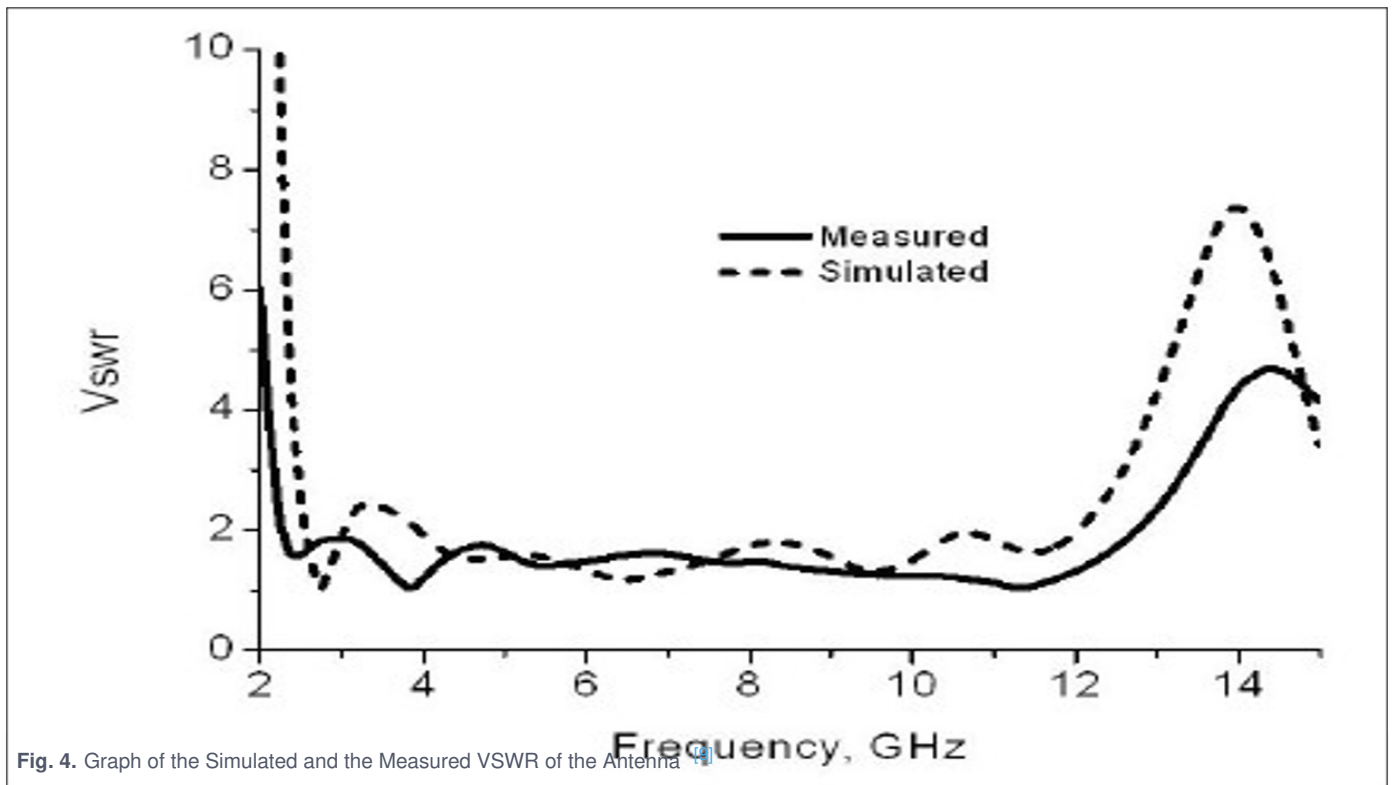
**Fig. 2.** 3-Dimensional view of the Miniaturised Antenna [\[9\]](#)



The disadvantage of using an RF absorber is that it could produce conductive cavities that will oscillate if simulated at one of its resonant frequencies, whereby E and H fields are being introduced across the cavity and can seriously affect the circuit performance [9].

Following the same procedure as in their earlier paper presented in 2009, it can be seen from the graph below that there is a good correspondence between the simulated and the measured VSWR.





The antenna was able to achieve a high impedance bandwidth of about 10.5GHz (2.26-12.76GHz) for a Voltage Standing Wave Ratio less than or equal to 2. The gain, as measured, varies from -3.4dBi to -4.5dBi over the Ultra-wideband ranging from 3.1-10.6GHz. A unidirectional radiation pattern was achieved at all frequencies, but it was observed that the ratio of main lobe to side lobe was greater than 10dB at higher frequencies such as 7-10GHz and a little bit smaller at lower frequencies due to the small size of the metallic cavity compared to the operating wavelength. Figures 5, 6, 7, and 8 show the radiation patterns in the E and H planes, respectively, at 7GHz and 10GHz as measured by [9].

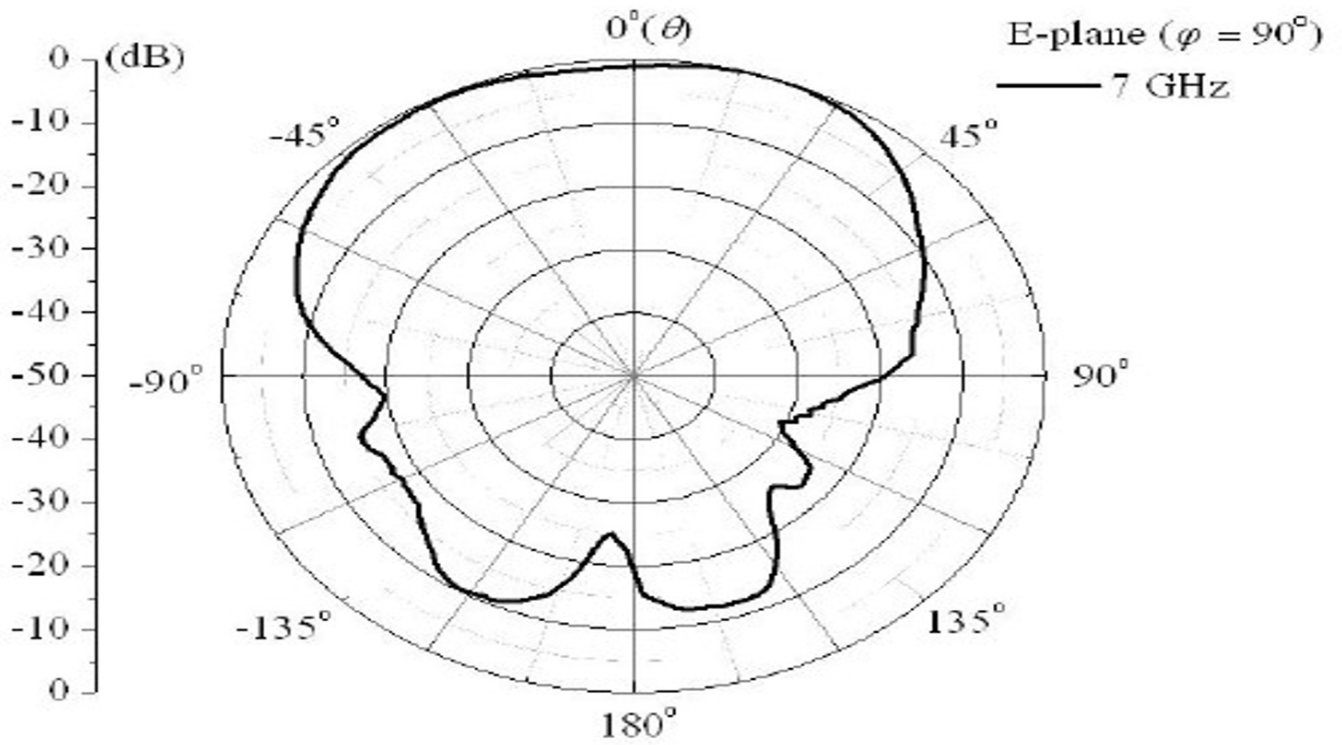


Fig. 5. Measured E-plane radiation pattern of the antenna at 7GHz [9]

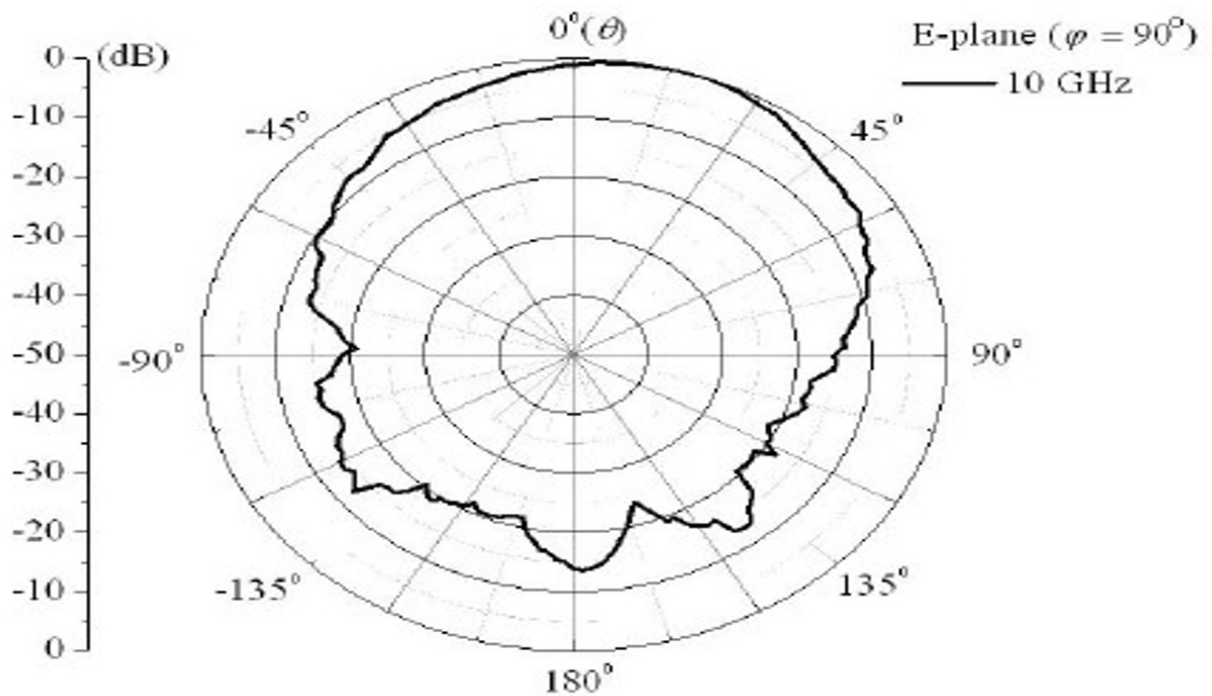


Fig. 6. Measured E-plane radiation pattern of the antenna at 10GHz [9]

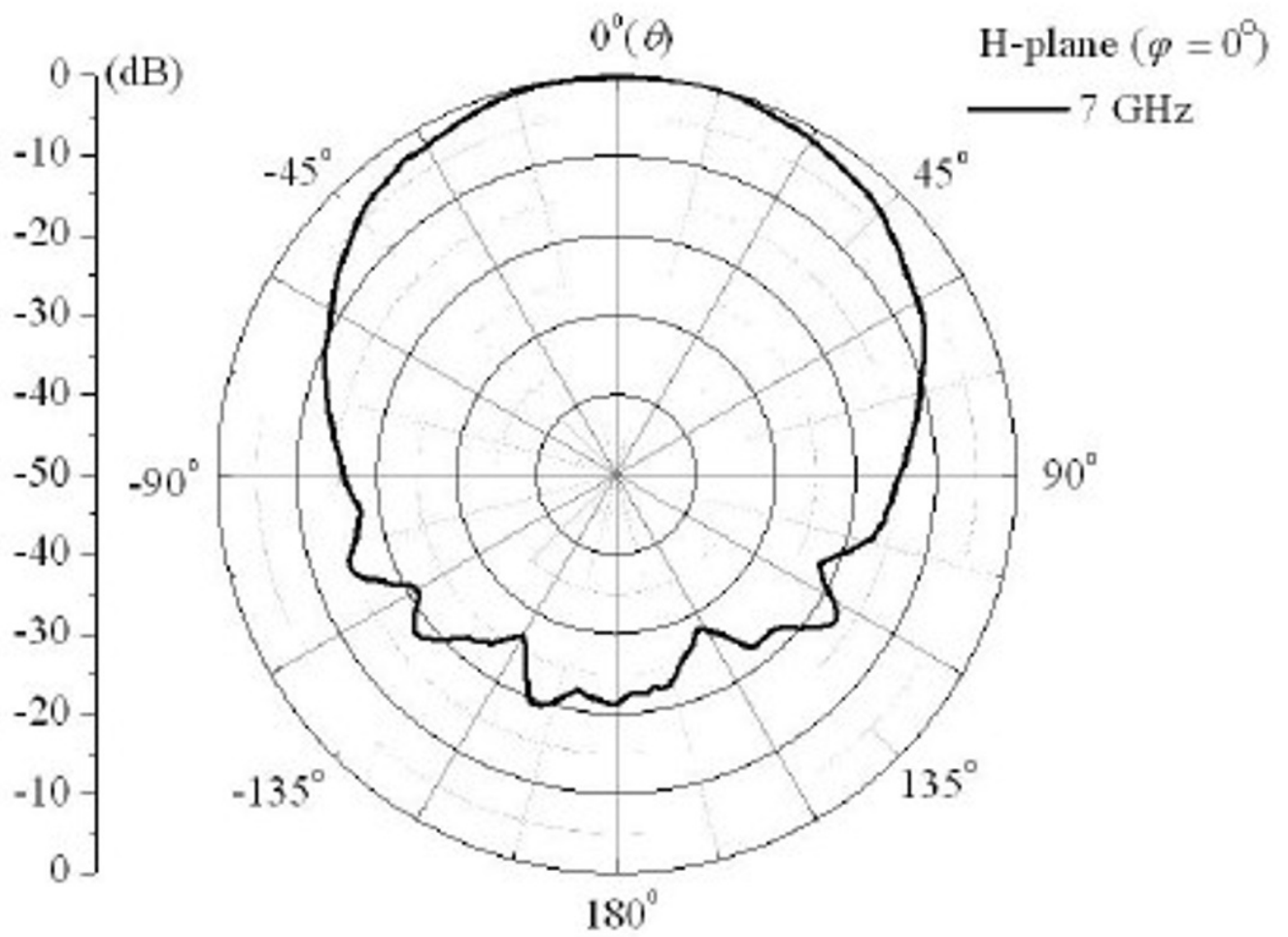


Fig. 7. Measured H-plane radiation pattern of the antenna at 7GHz [9]

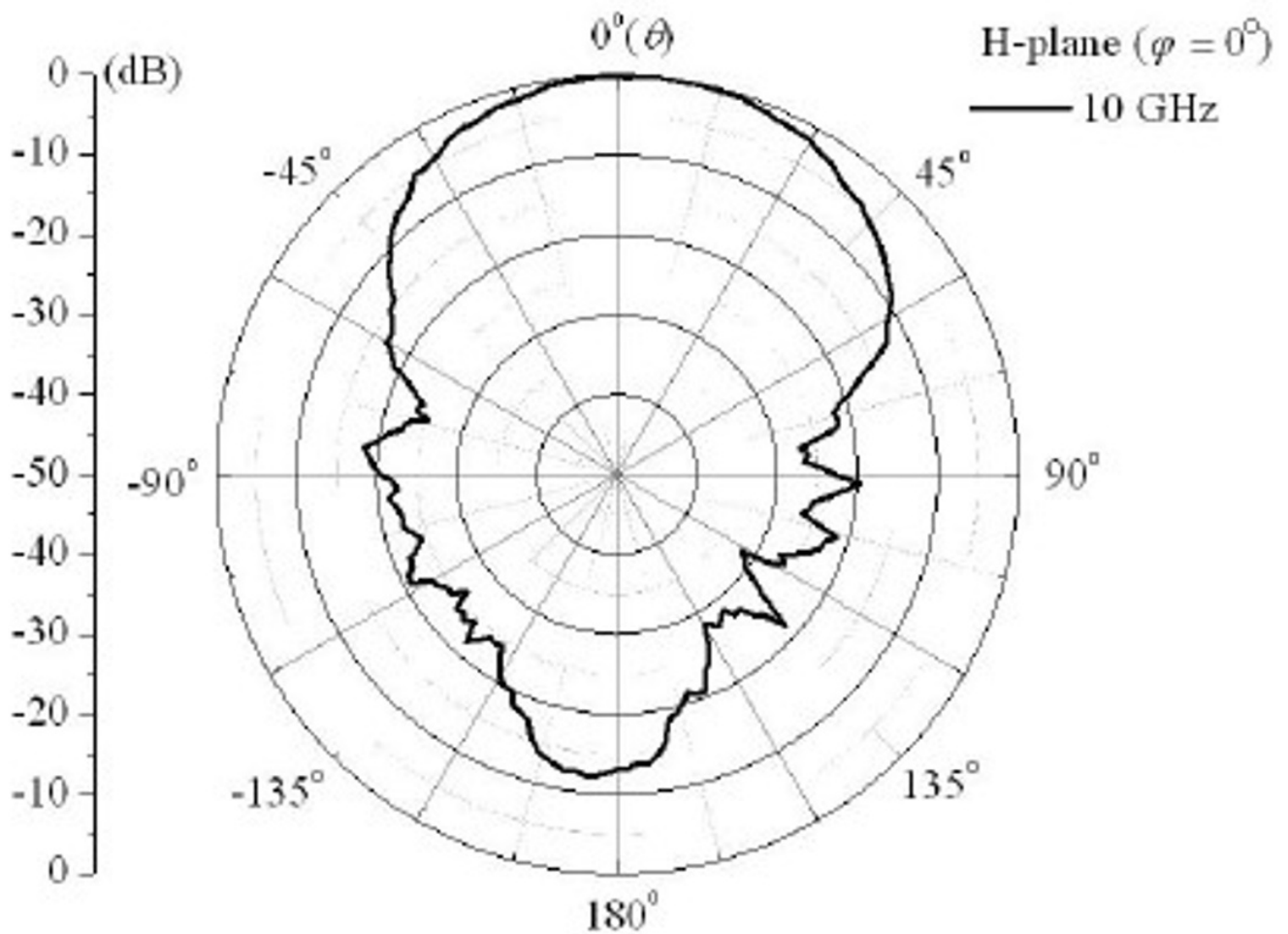


Fig. 8. Measured H-plane radiation pattern of the antenna at 10GHz [9]

### Increasing the Gain of a Semiconductor Slot UWB Antenna Using FSS

As part of gaining more insights in the research area, a review was carried out on a paper presented by [15] on how to increase the gain of a semi-conductor slot UWB antenna using a multi-layer FSS reflector. The multi-layer Frequency Selective Surface (FSS) provides an appropriate reflection phase to act as a reflector, and it is able to improve the slot antenna gain. The overall performance of the UWB system should be put into consideration when designing UWB antennas, and one way to improve the system performance is to increase antenna gain at the receiver end [15]. A directional transmitting antenna helps to reduce emissions in unwanted directions.

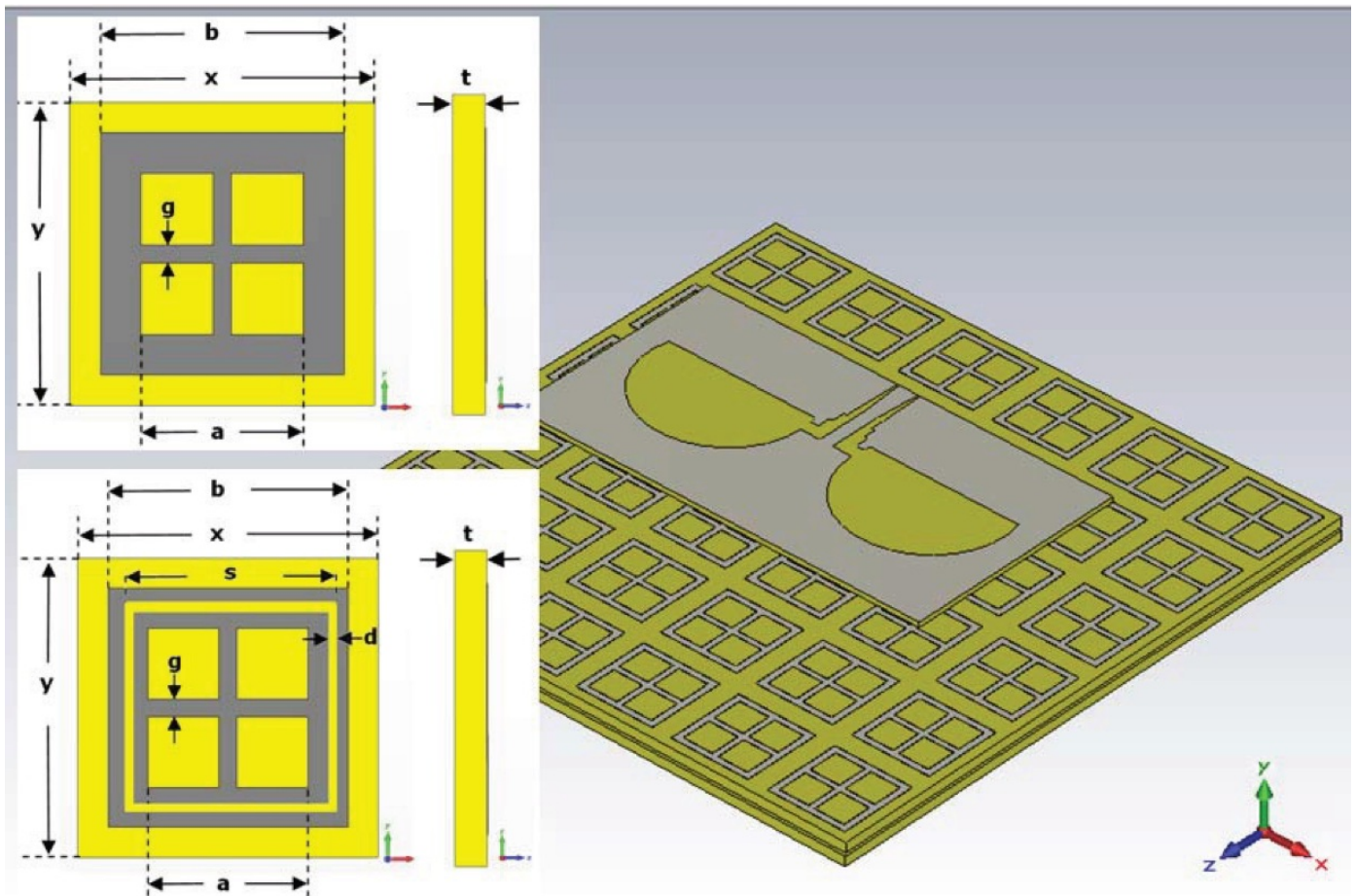


Fig. 9. Semi-circular Slot Antenna over the Dual-layer FSS Reflector [15]

Line-of-sight communication systems (LOS) and quasi-LOS are the most important cases in UWB short-range communications. Most directional antennas are larger than omni-directional antennas, whereas several UWB systems require small, easily integrable, and low-cost antennas [15].

[15], made use of the FSS reflector concept and tested this idea on UWB slot antennas. A semi-circular slot antenna (SSA) was taken as the reference antenna, and a way to improve the gain of the semi-circular slot antenna was established while maintaining an impedance bandwidth. By combining step and taper transitions to the CPW feed line, a better matching to the resonant modes of the semi-circular conductor was obtained. A percentage bandwidth of 118% was obtained, which shows that the 10dB return loss extended from 3GHz to 11.6GHz. The FSS unit plays an important role in the design of a reflector. It is made of 2 layers; the first layer combines cross dipole and loop elements, while the second layer comprises similar unit cells with an additional slit in the square loop. A stop band from 3.5GHz to 11.5GHz was obtained as a result of the simultaneous optimization of both layers. The CST Microwave Studio software was used to carry out the simulation, and the predicted results were obtained. There is an increase over the entire frequency band in the antenna gain with the use of a dual-layer FSS reflector. The reflection coefficient and the gain of the antenna with and without the FSS reflector, as predicted by [15], are shown in Figure 10 and Figure 11, respectively.

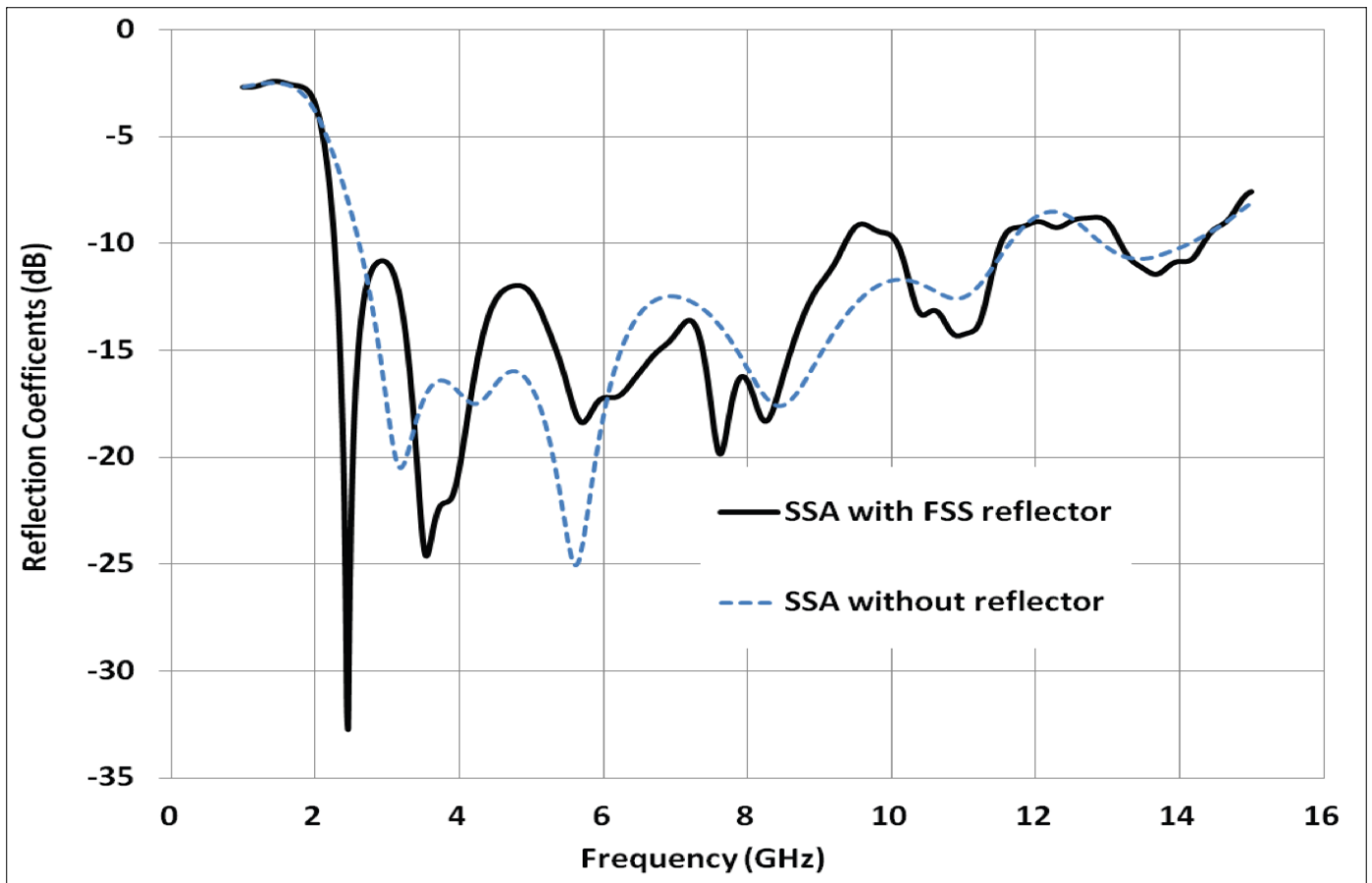


Fig. 10. Input Reflection Coefficient of the SSA with and without the Reflector [15]

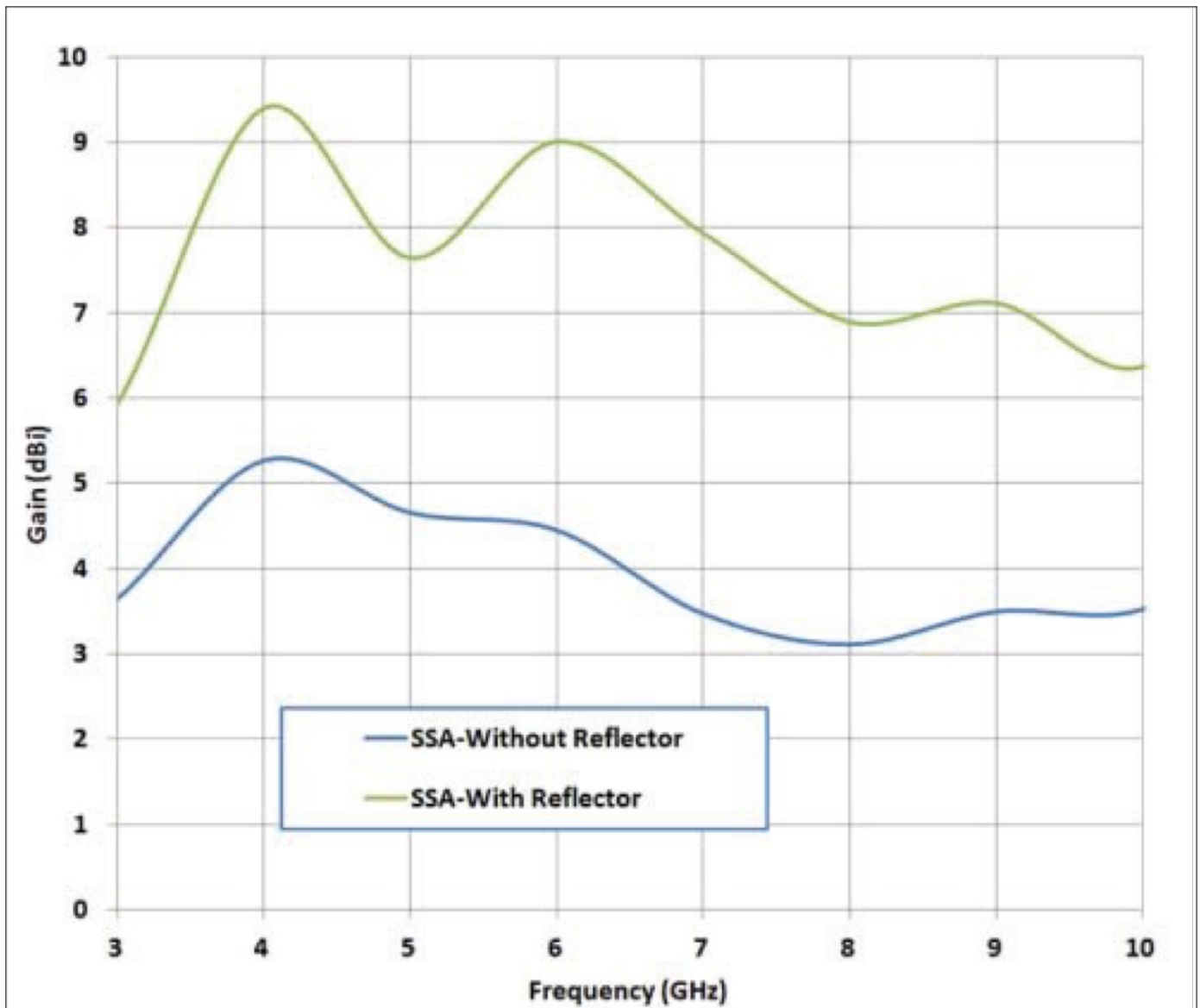


Fig. 11. Gain of the SSA with and without a reflector [15]

The return loss of the antenna was not much affected by the reflector, but a good impedance match was maintained by the antenna with the reflector, with a return loss greater than  $-9\text{dB}$  over the entire UWB frequency band. In terms of radiation, the antenna gave a bi-directional radiation pattern similar to that of a slot antenna; the radiation pattern became uni-directional with the addition of the reflector.

Different types of papers on ultra-wideband antenna designs have been reviewed. The major challenge in most antenna designs is the emission of energy as a result of back radiation, which makes the systems not completely directional. Ways to avoid this emission of energy were discussed, including the addition of a metallic cavity underneath the monopole-like antenna or the use of a reflector.

### 3. Materials and Methods

Section two intended to help the reader establish an understanding of what has been done by other researchers in this area. This section focuses on several methodologies adopted for the successful completion of this study. The research approach adopted was based on literature with the highest level of methods and developments. A descriptive and quantitative approach was used. The materials used for the simulation of the prototype are a Computer-Aided Design (CAD) software – CST Microwave Studio, a Transient Solver – 3D electromagnetic simulator, an FR4 substrate with a dielectric constant of 4.3, a 50Ω SMA connector, calibration kits, and a network analyzer. Investigations carried out on the input impedance and radiation pattern of the UWB antenna are presented in this section.

The proposed antenna was implemented with a low-cost FR4 substrate with a dielectric constant  $\epsilon_r = 4.3$  and a thickness  $h = 1.6\text{mm}$ . Two models were simulated; the components of the first model are ground plane, substrate, inner patch, and an inner feeder. The only difference between the first and the second model is the addition of another ground plane to serve as a reflector, so as to increase the directivity of the antenna. The antenna is made up of a rectangular aperture carved out from the ground plane of a printed circuit board (PCB) and a T-shaped stub for excitation<sup>[10]</sup>. The antenna and the feeding structure are implemented on the same plane, which makes the fabrication of the antenna cost-effective and very easy. A microstrip transmission line designed with a characteristic impedance of 50Ω and a subminiature connector was used for the termination during the measurement process. A compact aperture area of 13x23mm<sup>2</sup> is achieved. A quarter-wavelength is greater than the dimensions for the lowest UWB frequency (3.1GHz).

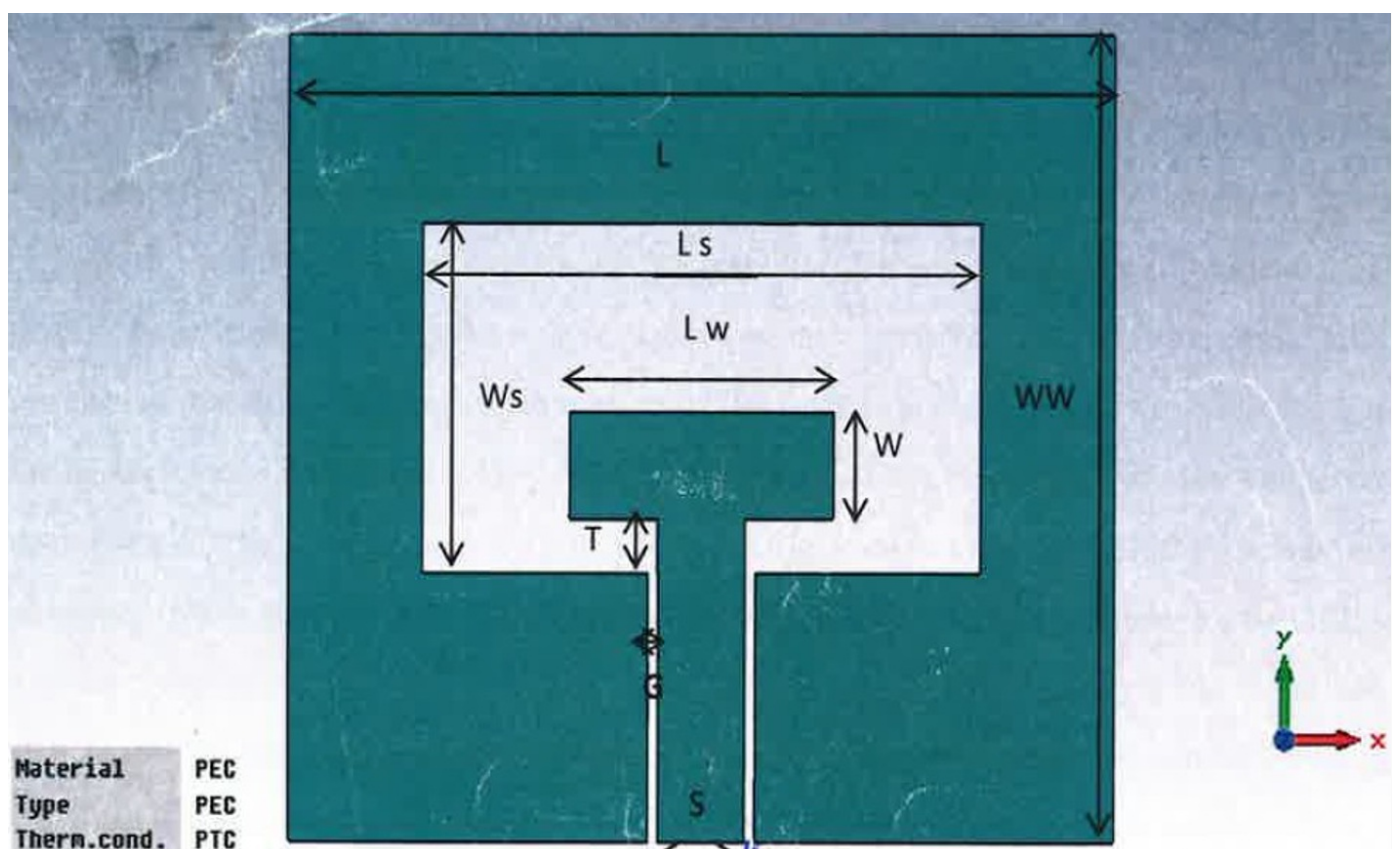


Fig. 12. Geometry and Configuration of the Proposed Antenna (Lin & Hung, 2006)



The geometry and configuration of the proposed antenna are shown in Figure 12. The length  $L_w$ , the width  $W$ , and the extrusion depth  $T$  are the only three parameters of the T-shaped stub (Lin and Hung, 2006). The design parameters are  $W_s=13\text{mm}$ ,  $L_s=23\text{mm}$ ,  $T=2\text{mm}$ ,  $W=4\text{mm}$ ,  $L=34\text{mm}$ ,  $W_w=30\text{mm}$ ,  $S=3.6\text{mm}$ ,  $G=0.4\text{mm}$ ,  $L_w=10.8\text{mm}$ ,  $S_1=12$ ,  $t_{\text{patch}}=0$ , and  $t_{\text{sub}}=1.6\text{mm}$ . The dimensions of the components were calculated. **Table 1** shows the dimensions used for the components.

**Table 1.** Table showing the dimensions used for the components (Source - The Authors)

Components	$X_{\min}$	$X_{\max}$	$Y_{\min}$	$Y_{\max}$	$Z_{\min}$	$Z_{\max}$
Inner patch	$-L_w/2$	$L_w/2$	$T$	$T+W$	0	$t_{\text{patch}}$
Inner feeder	$-S/2+G$	$S/2-G$	$-S_1$	$T$	0	$t_{\text{patch}}$
Substrate	$-L/2$	$L/2$	$-S_1$	$W_w-S_1$	$-t_{\text{sub}}$	0
Ground	$X_p(1)$	$X_p(2)$	$Y_p(1)$	$Y_p(2)$	0	0

A well-designed model was obtained after using the above dimensions for the individual components. After that, a waveguide port was added to it before simulation commenced. The dimension of the port is shown in **Table 2**.

**Table 2.** Table showing the dimensions of the waveguide port, (Source - The author)

Port	$X_{\min} = -S/2-G-t_{\text{sub}}*3$	$X_{\max} = S/2+G+t_{\text{sub}}*3$	$Z_{\min} = -1.6-5$	$Z_{\max} = 7$

### Investigations on Input Impedance and Radiation Pattern using the UWB Antenna with a Reflector

Investigations were carried out using the antenna with a reflector, which comprises a substrate, an inner feeder, an inner patch, a ground plane, and an additional ground plane that was added to it and serves as a reflector. The dimensions of the inner feeder, inner patch, substrate, and the ground plane were kept constant as in the previous model, while the dimensions of the reflector were added. Table 1 shows the dimensions of the reflector where  $L_f=60\text{mm}$ ,  $L_f\text{offset}=25\text{mm}$ , and  $W_f=60\text{mm}$ .

**Table 3.** Table showing the Dimensions of the Reflector (Source - The authors)

Component	$U_{\min}$	$U_{\max}$	$V_{\min}$	$V_{\max}$	$W_{\min}$	$W_{\max}$
Reflector	$-W_f/2$	$W_f/2$	$-L_f\text{offset}$	$-L_f\text{offset}+L_f$	$-df$	$df$

The starting point for this investigation, after reviewing different literatures, was to calculate the distance at which the reflector would be positioned to the substrate. This reflector was placed at a distance of a quarter-wavelength to the substrate. The value of the quarter wavelength was calculated using the formula:

$\lambda = c/f$  where  $c = 3 \times 10^8$  m/s and  $f$  is the centre of the frequency band.

Therefore,  $f = (3.1 + 10.6)/2 = 6.85\text{GHz}$

$$\lambda = 3 \times 10^8 \div 6.85 \times 10^9 = 0.0437\text{m}$$

$$\text{Quarter wavelength} = \frac{\lambda}{4} = \frac{0.0437}{4} = 0.0109\text{ m}$$

$$0.0109\text{m} = 10.9\text{mm}$$

This value is an estimated value of the quarter-wavelength at which the reflector was placed to the substrate, as the effect of the substrate ( $\epsilon_r = 4.3$ ) is ignored. Figure 13 shows the picture of the model with the reflector ready for simulation.

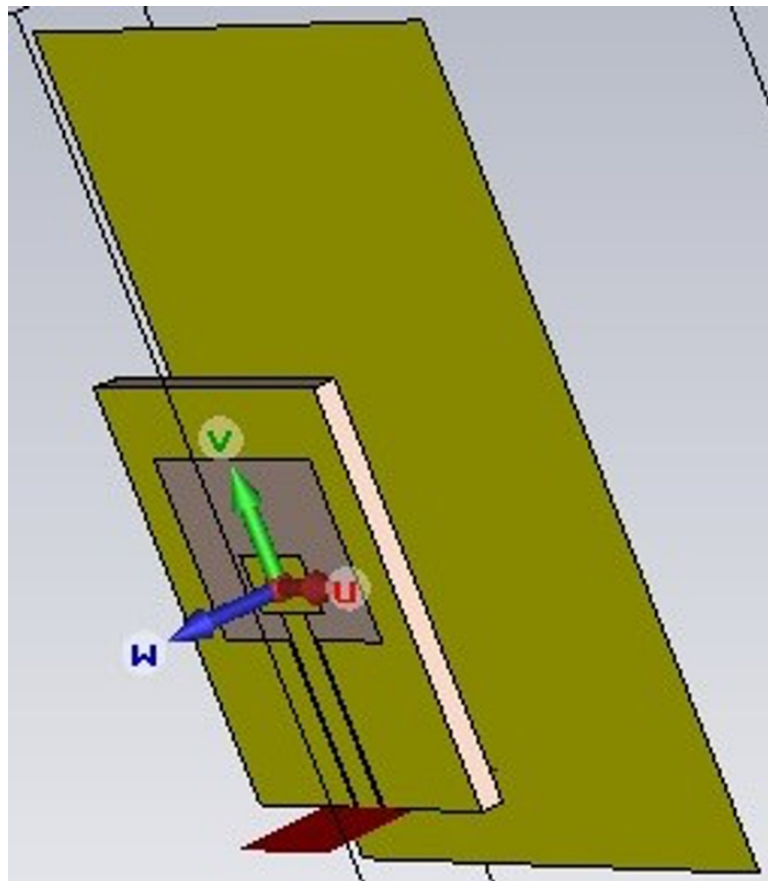


**Fig. 13.** Picture of the Designed Model of the Proposed Antenna with a Reflector  
(Source -The Authors)

The designed proposed antenna with a reflector is now ready for the optimization process. The effects of parameters  $W$ ,  $T$ , and  $L_s$  on the input impedance were carried out using the parameter sweep option of the time domain solver, just as it was done in the case of the first model. Figures 14 – 16 show the effects of the variation of the parameters.

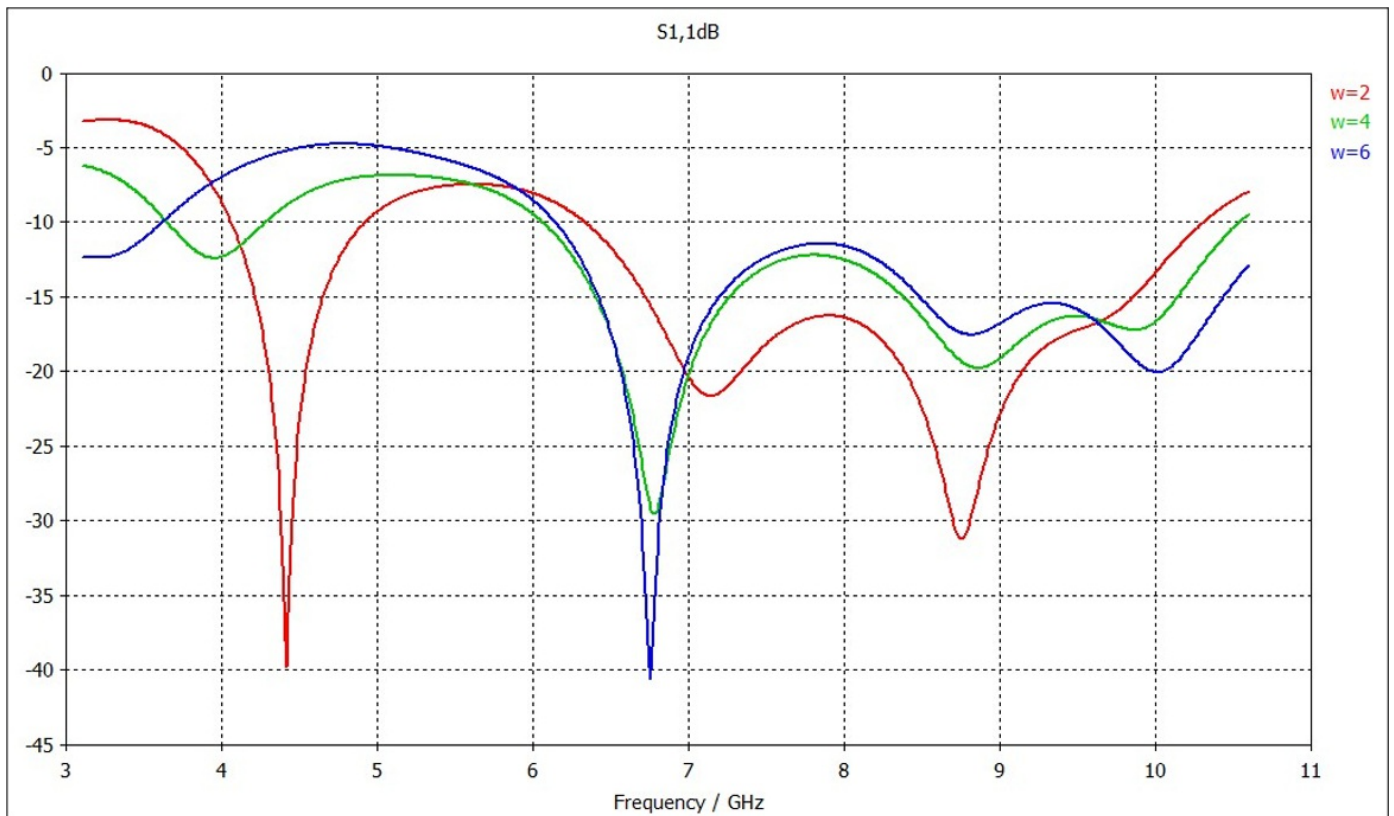


Fig. 14. Effects of the Variation of Width W on the Model with a Reflector (Source - The Authors)

The dimension of other parameters is kept constant. Figure 14 illustrates the return loss of the designed antenna when we varied the width W of the T-shaped stub. When the value of W was reduced to 2mm, the return loss increased at the starting frequencies of 3.1GHz to 4.1GHz, middle frequencies of 5.6-7GHz, and higher frequencies of 9.6-10.6GHz, but it decreased between 4.1GHz to 4.5GHz, 6.8GHz to 7.3GHz, and 8.88GHz to 9.6GHz. The antenna transmits less power when the return loss increases, and it radiates more energy when the return loss decreases.

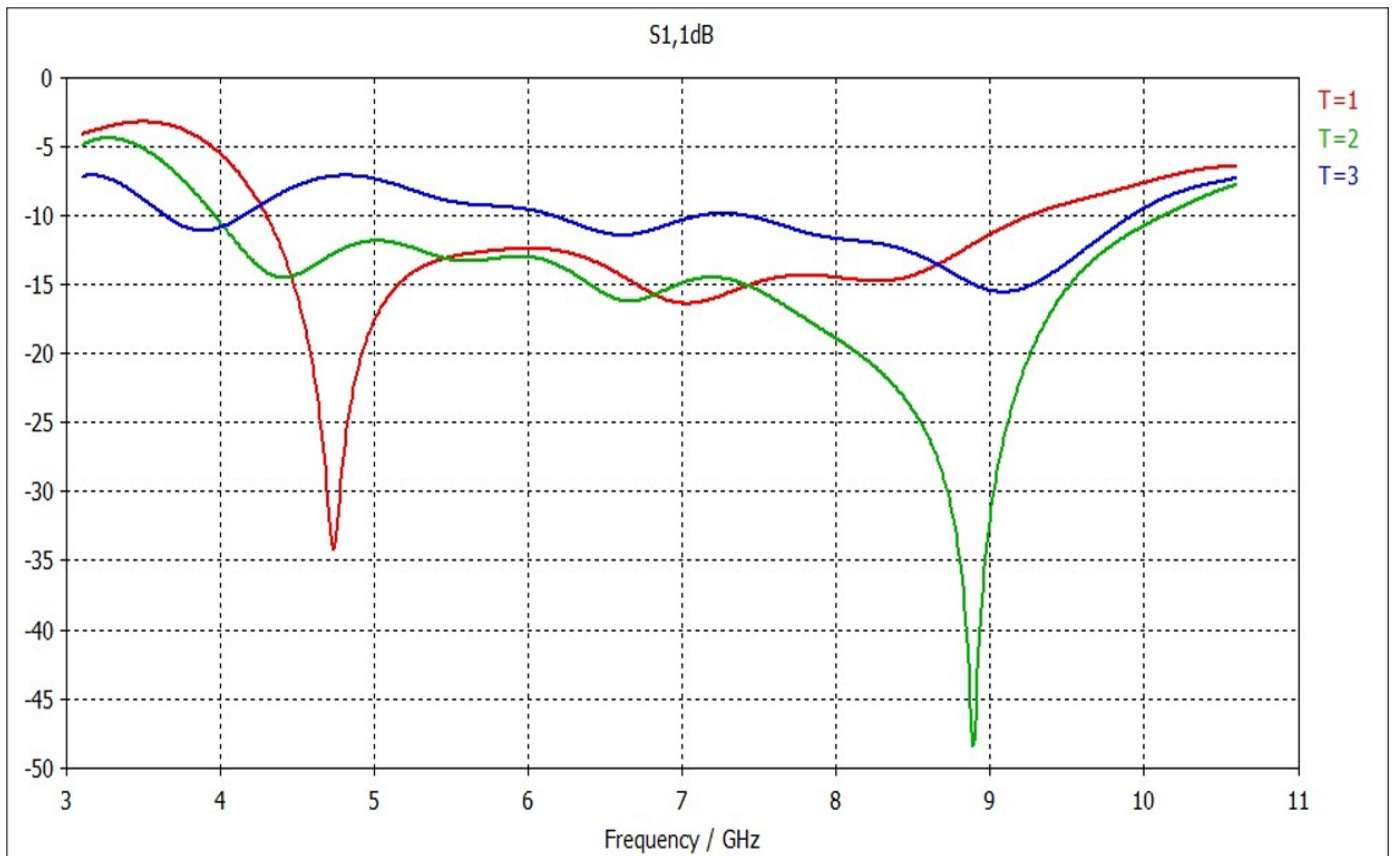


Fig. 15. Effects of the Variation of Extrusion Depth T on the Model with a Reflector (Source - The Authors)

The above Figure 15 shows the effects of the variation of the extrusion depth T on the designed antenna. The reduction of T aggravated the return loss between 3.1GHz to 4.2GHz, 5.5GHz to 6.9GHz, and 7.5GHz to 10.6GHz, but it decreased between 4.5GHz to 5.4GHz. The return loss is greater over the entire bandwidth when the value of T is increased. Less power is transmitted at frequencies of 4.5GHz to 5.4GHz when T decreases.

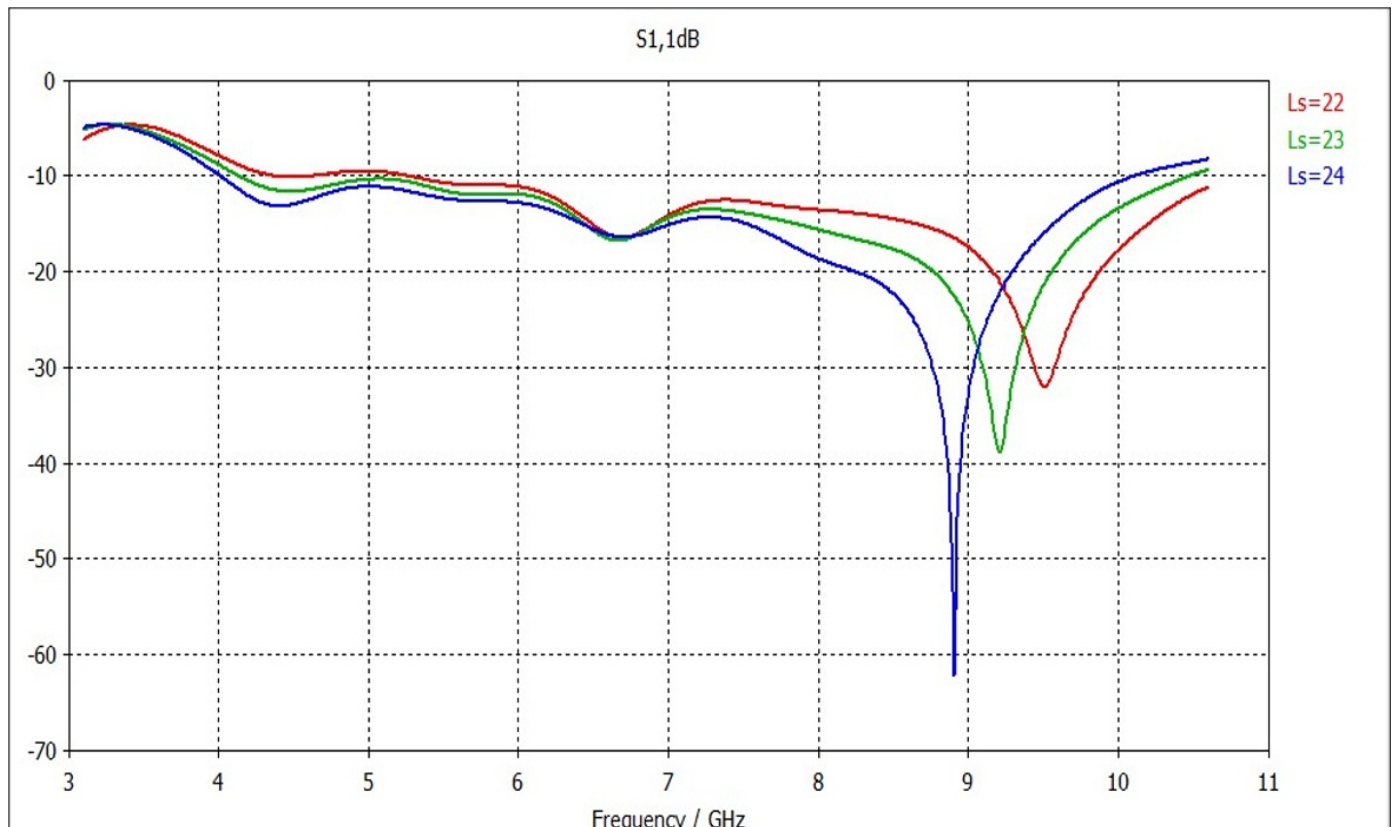
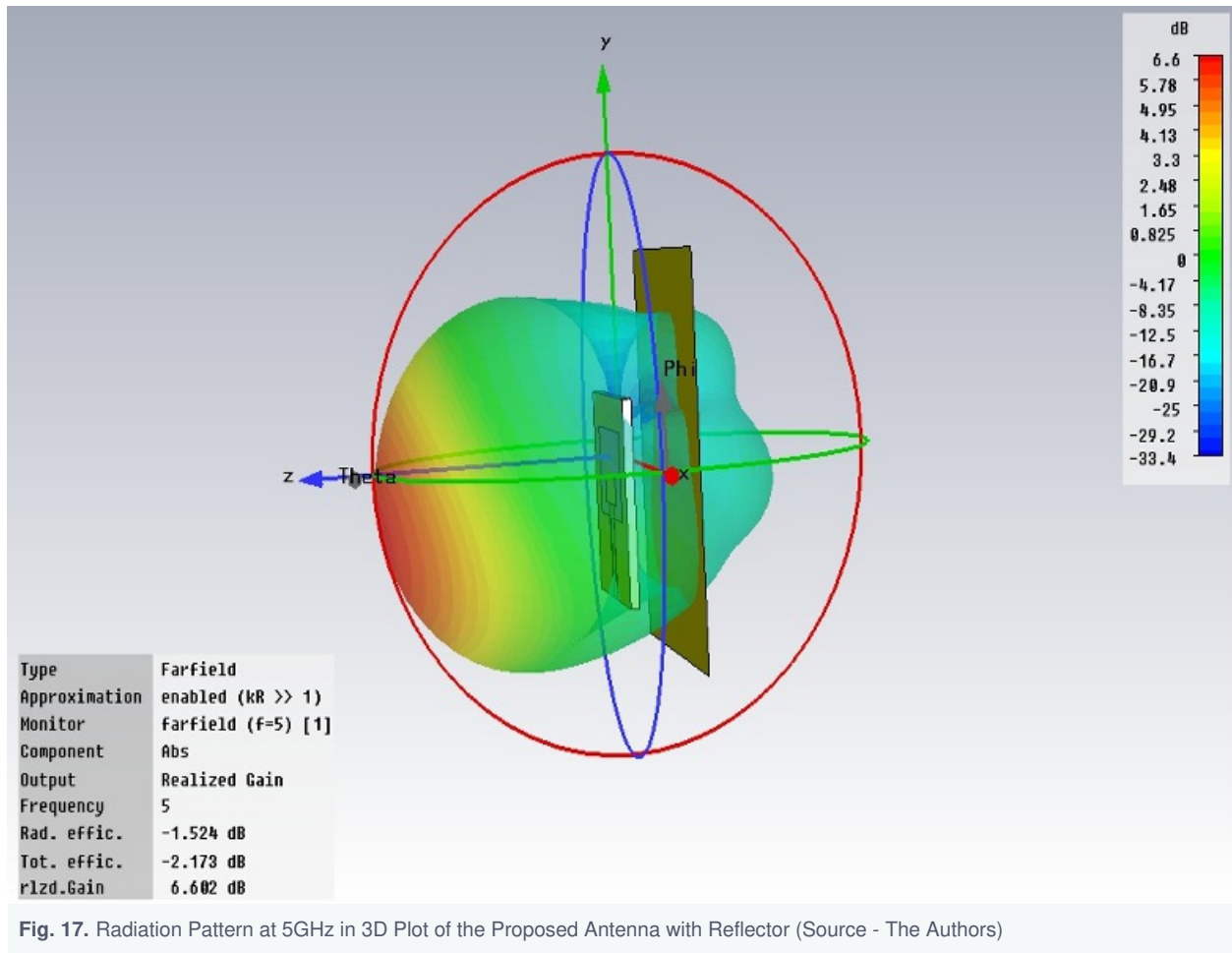


Fig. 16. Effects of the Variation of Length  $L_s$  on the Model with a Reflector (Source - The Authors)

Figure 16 illustrates the variation of the length of the antenna aperture. It can be deduced from the illustration that an increase in length  $L_s$  influences higher frequencies compared to the initial value of  $L_s$ , which is 23mm, as it brings about a great decrease in the return loss, while a decrease in  $L_s$  provokes an increase in the return loss from 3.1GHz to 6GHz and 7.2GHz to 9GHz. A high percentage of power is being transmitted by the designed antenna while less power is being radiated, and the bandwidth changes proportionally with the variation.

### Radiation Characteristics of the UWB Antenna with the Reflector

The designed UWB antenna exhibits a directional radiation pattern except at lower frequencies of 3.1-4.4GHz, where the impedance matching seems poor. The radiation pattern of the proposed antenna with reflector was implemented at 5GHz, 8GHz, and 10GHz. It is obvious from the plots that a more directional radiation pattern is obtained when compared to the initial model without the reflector. As seen in Figure 17, the realised gain achieved is 6.6dB, and gains of 0.825dB and -25dB are achieved in the y-plane and z-plane, respectively.



When compared to the radiation pattern obtained for the UWB antenna without a reflector at 5GHz, the realised gain is twice the realised gain of the antenna without a reflector, which implies good directivity, as an increase in gain brings about good directivity.

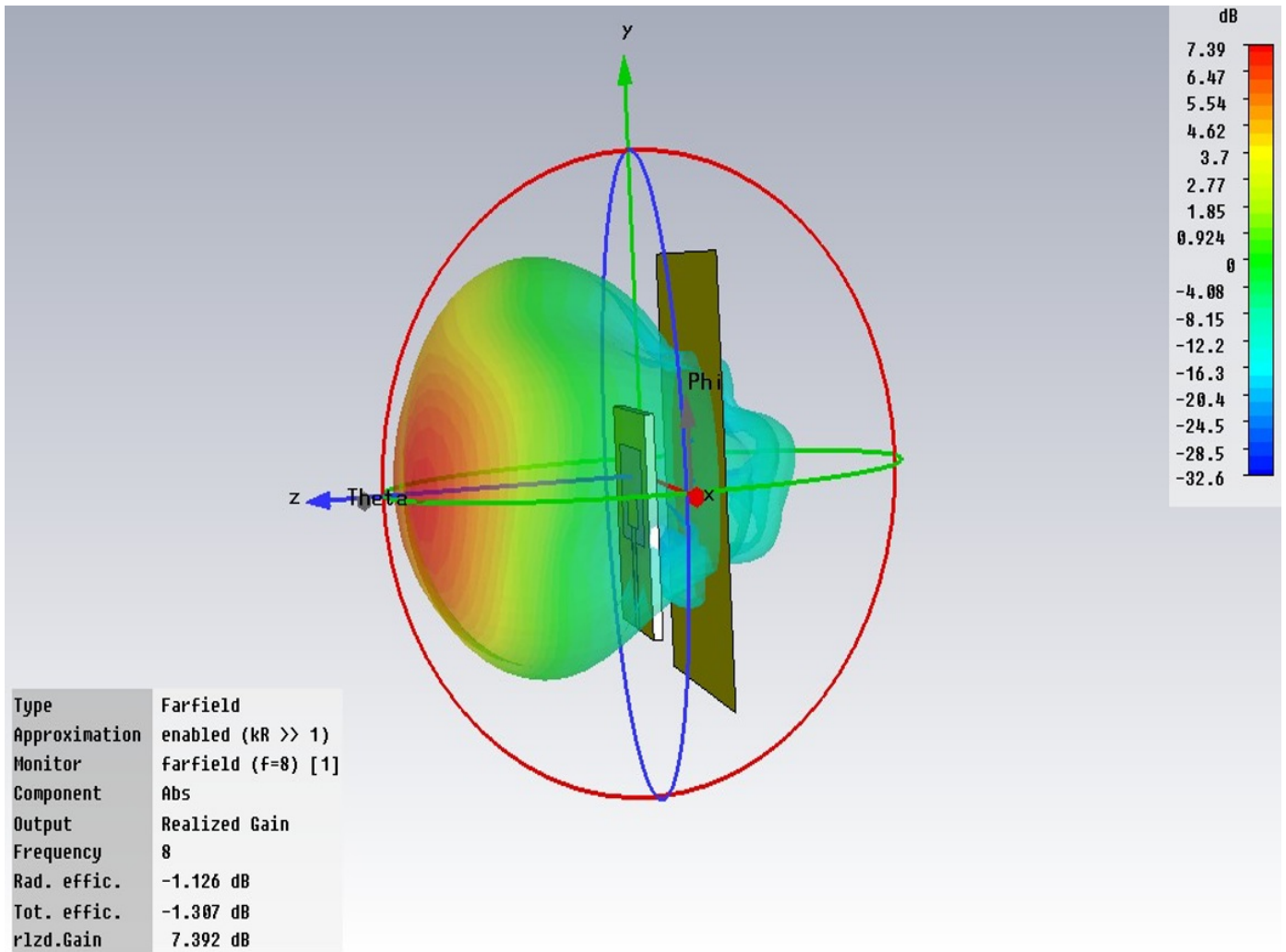


Fig. 18. Radiation Pattern at 8GHz in 3D Plot of the Proposed Antenna with Reflector (Source - The Authors)

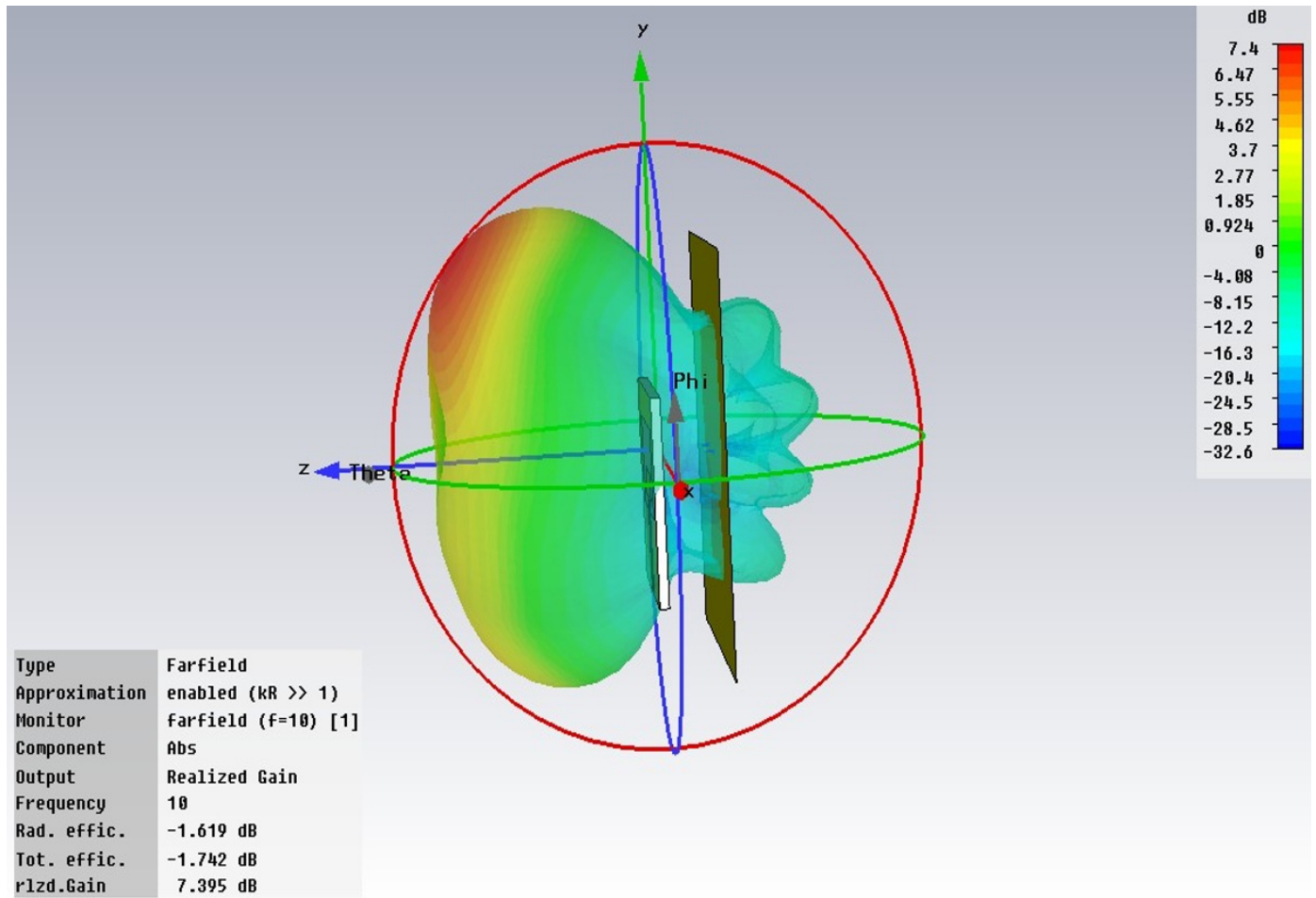


Fig. 19. Radiation Pattern at 10GHz in 3D Plot of the Proposed Antenna with Reflector (Source - The Authors)

There is not much difference between the realised gain at 8GHz and 10GHz. A realised gain of 7.392dB and 7.395dB is achieved at both frequencies, respectively. When compared to the gain of the UWB antenna without a reflector, it can be deduced that a directional radiation pattern is obtained.

#### 4. Results and Analysis

This section presents the results and analysis of the investigations carried out on the input impedance and radiation pattern of the proposed ultra-wideband (UWB) antenna. The simulated radiation patterns using polar plots at frequencies of 5GHz, 8GHz, and 10GHz are shown in Figures 20 - 22.



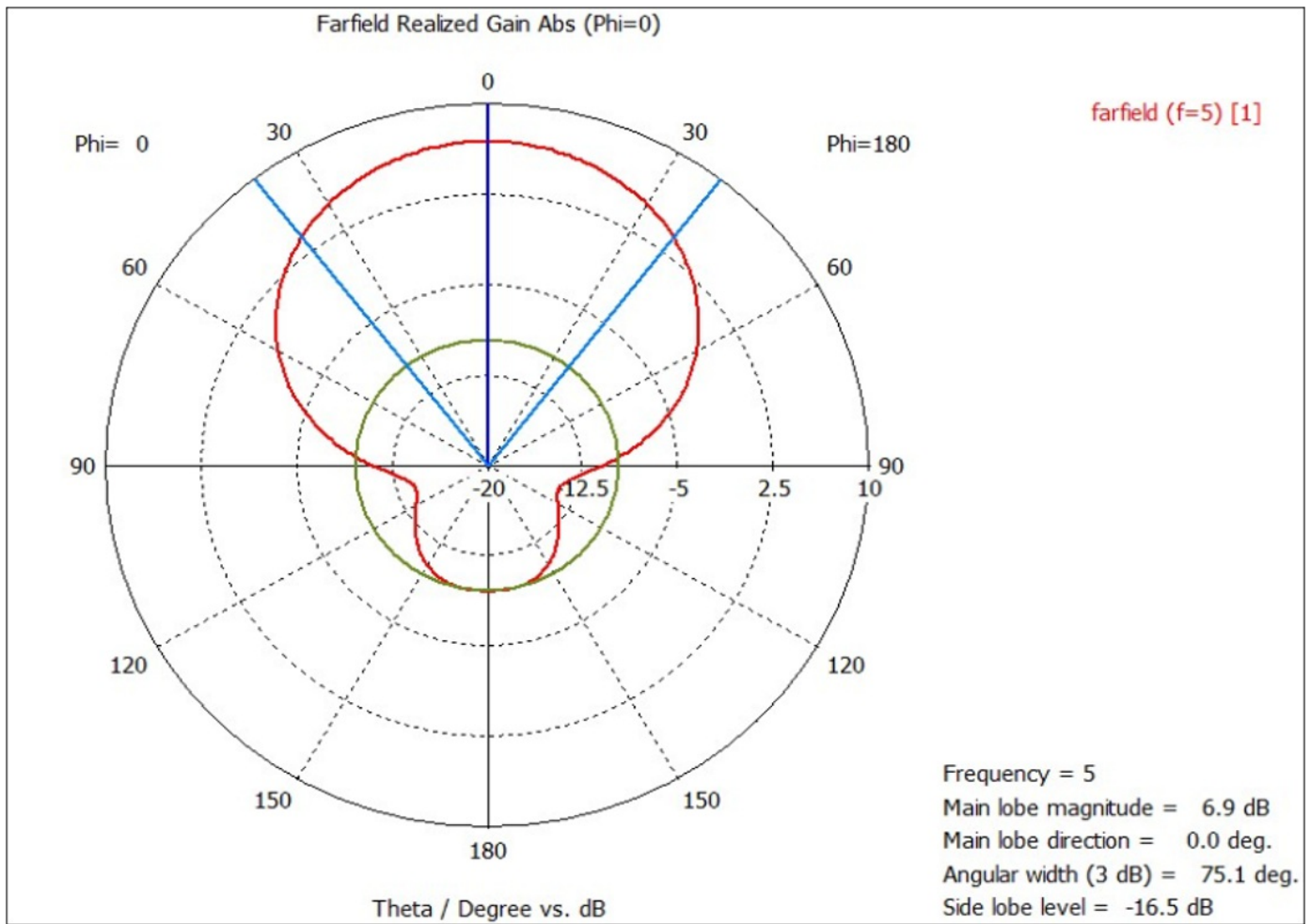


Fig. 20. Far-field realised gain at 5GHz (Source - The Authors)

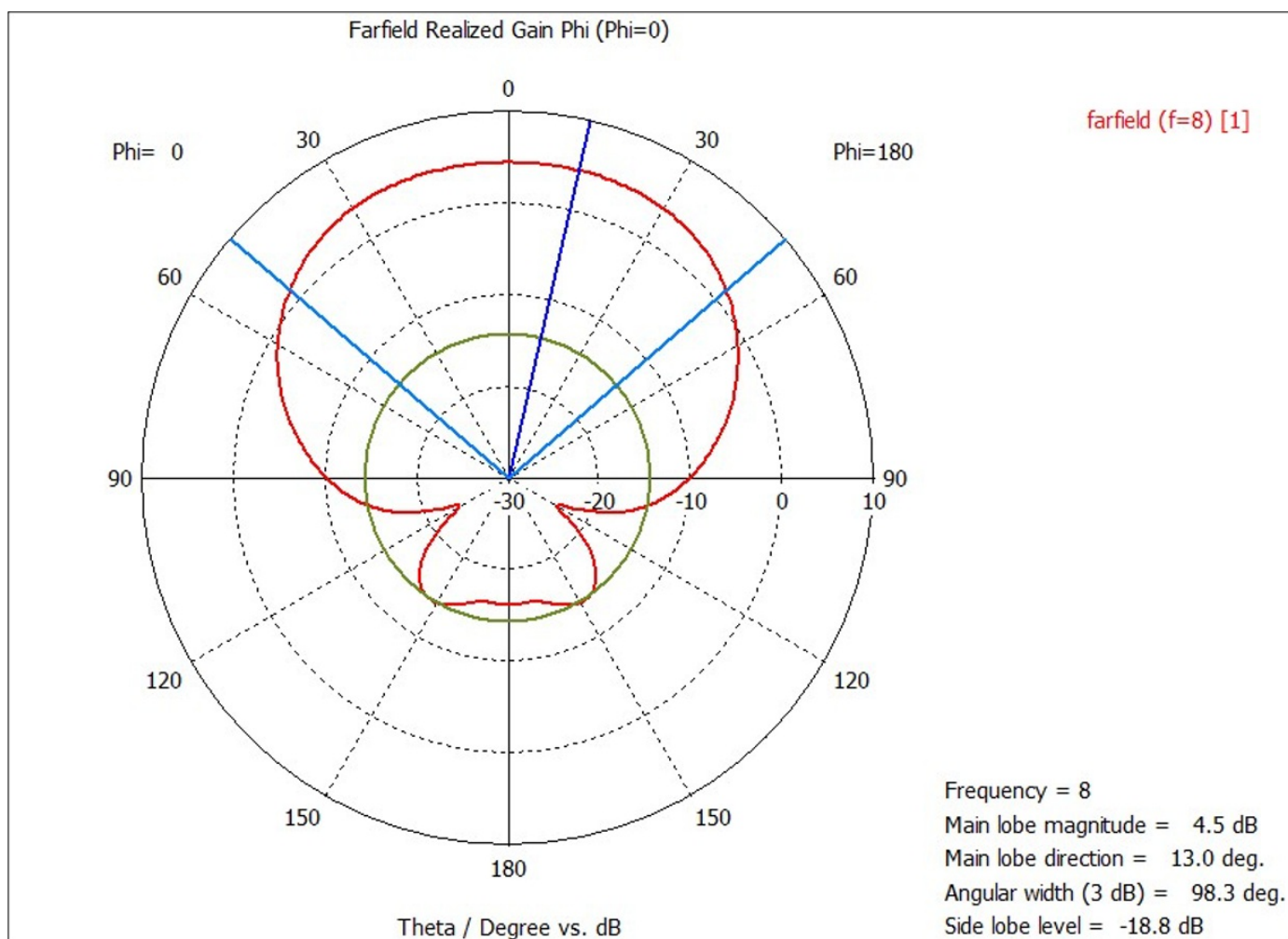


Fig. 21. Far-field Realized Gain at 8GHz (Source - The Authors)

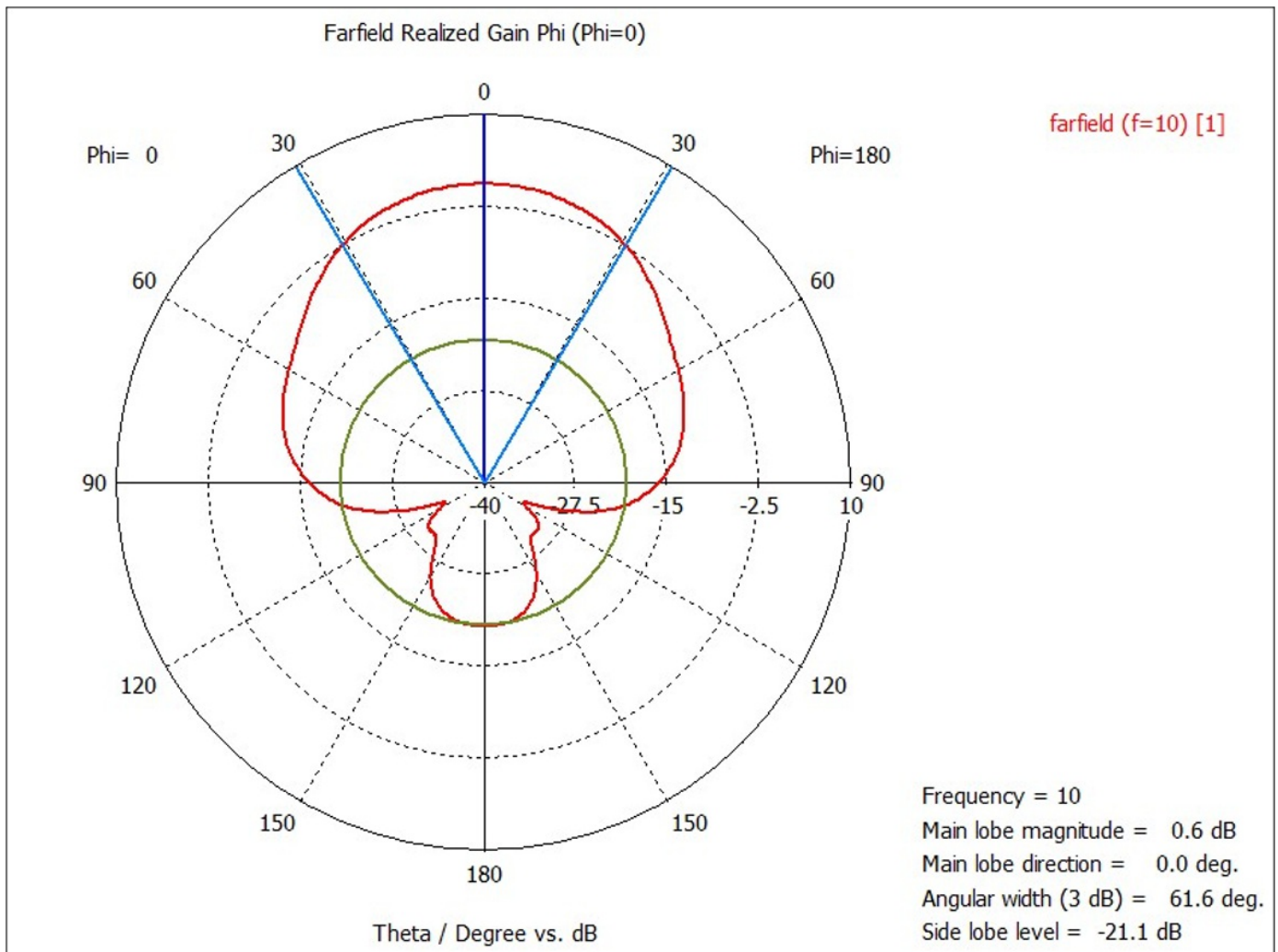


Fig. 22. Far-field Realised Gain at 10GHz (Source - The Authors)

After the optimization process has been completed using the commercial simulation tool, CST Microwave Studio software, it can be seen from the return loss plot shown in Figure 21 that the proposed antenna operates almost over the entire UWB band (3.1-10.6GHz) except at lower frequencies of 3.1-4GHz. The response of the designed UWB antenna starts at 3.1-10.6GHz, giving a good performance between 4GHz to 10.6GHz with an operational bandwidth of 6.6GHz. The input impedance is well matched as a return loss of 10dB is obtained between 4-10.6GHz. The return loss decreases even more at 4-5GHz and at 8-10GHz, which means that the proposed UWB antenna transmits a high percentage of its power while a very low power is reflected back.

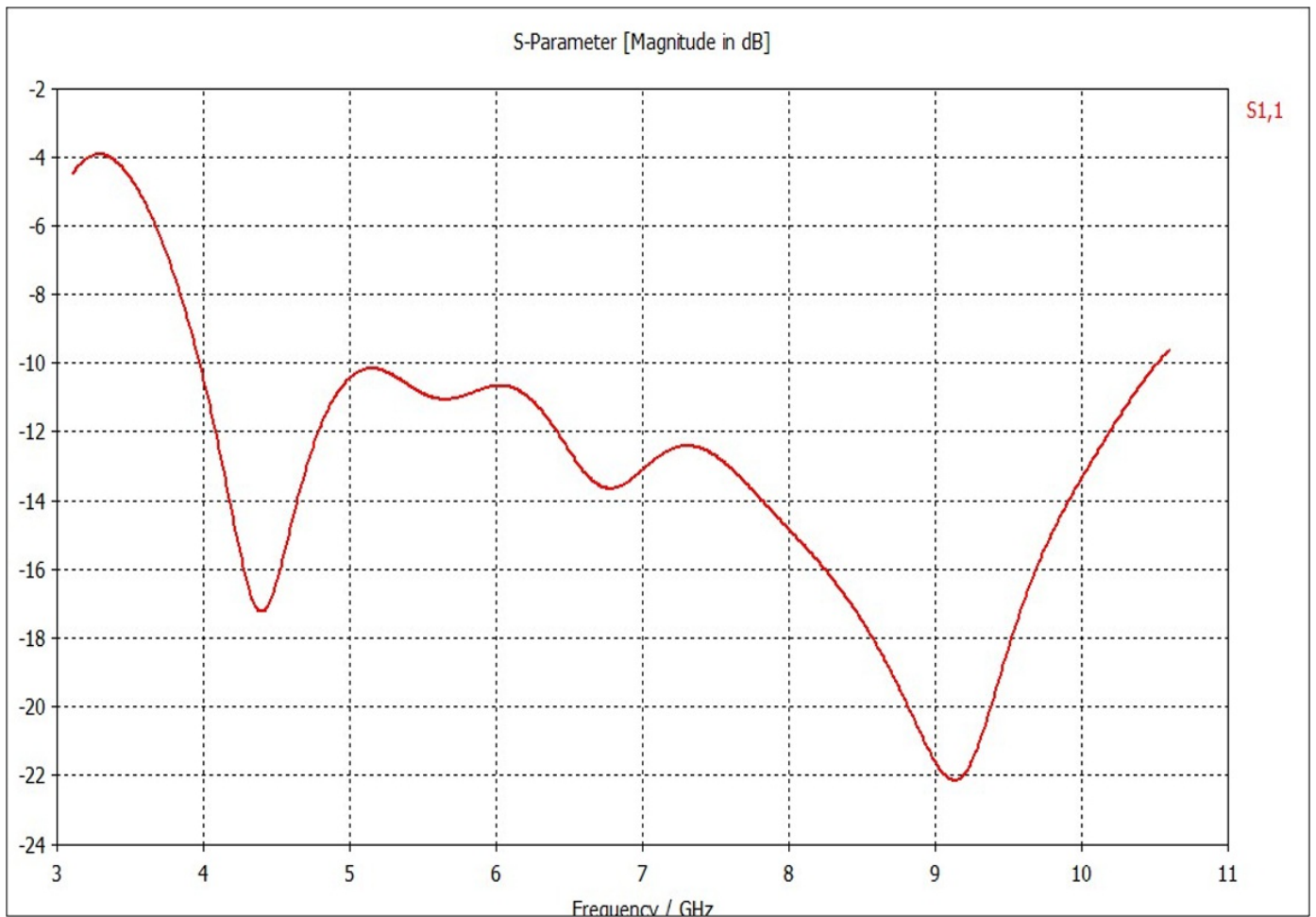


Fig. 23. Return Loss of the Designed Antenna (Source - The Authors)

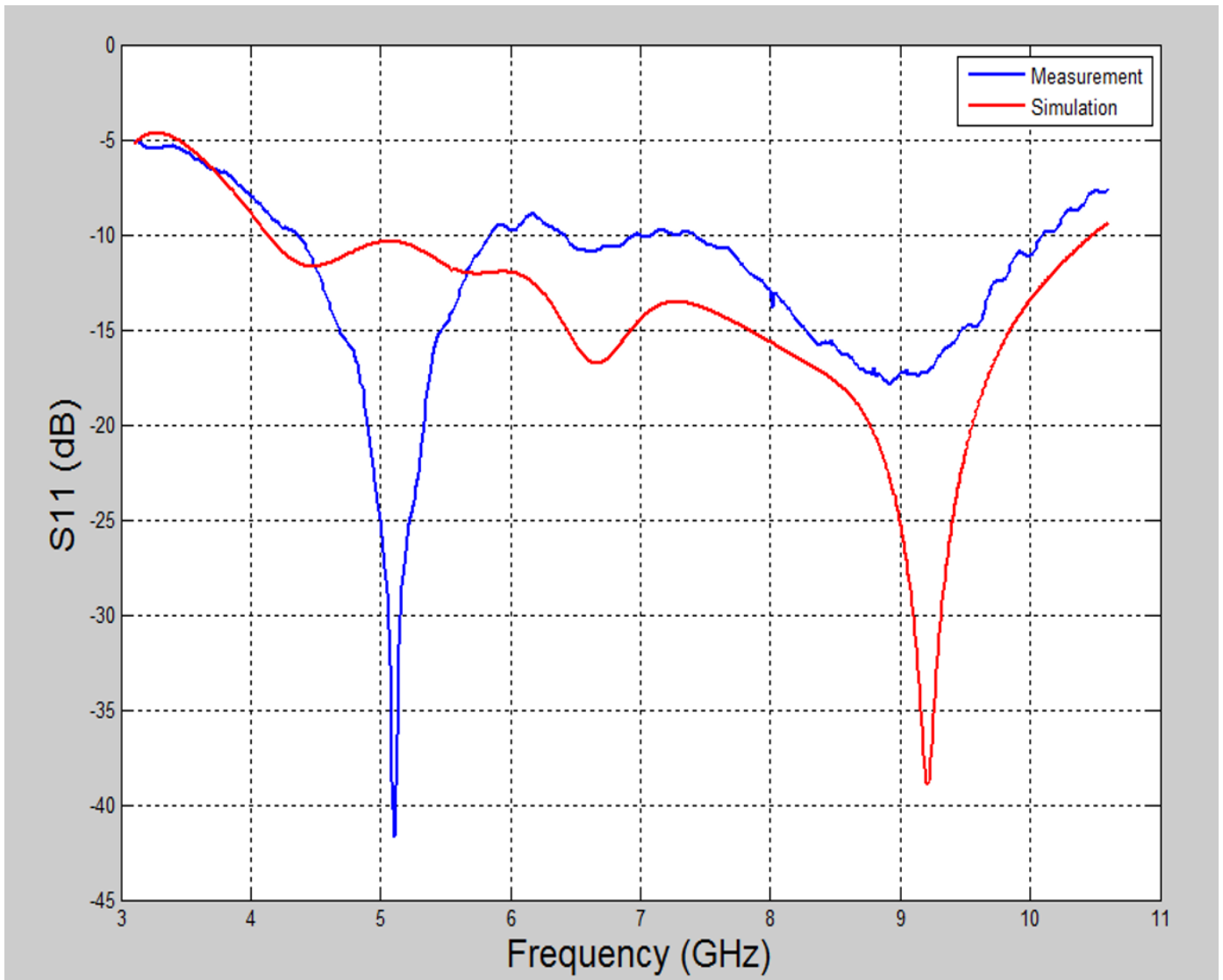
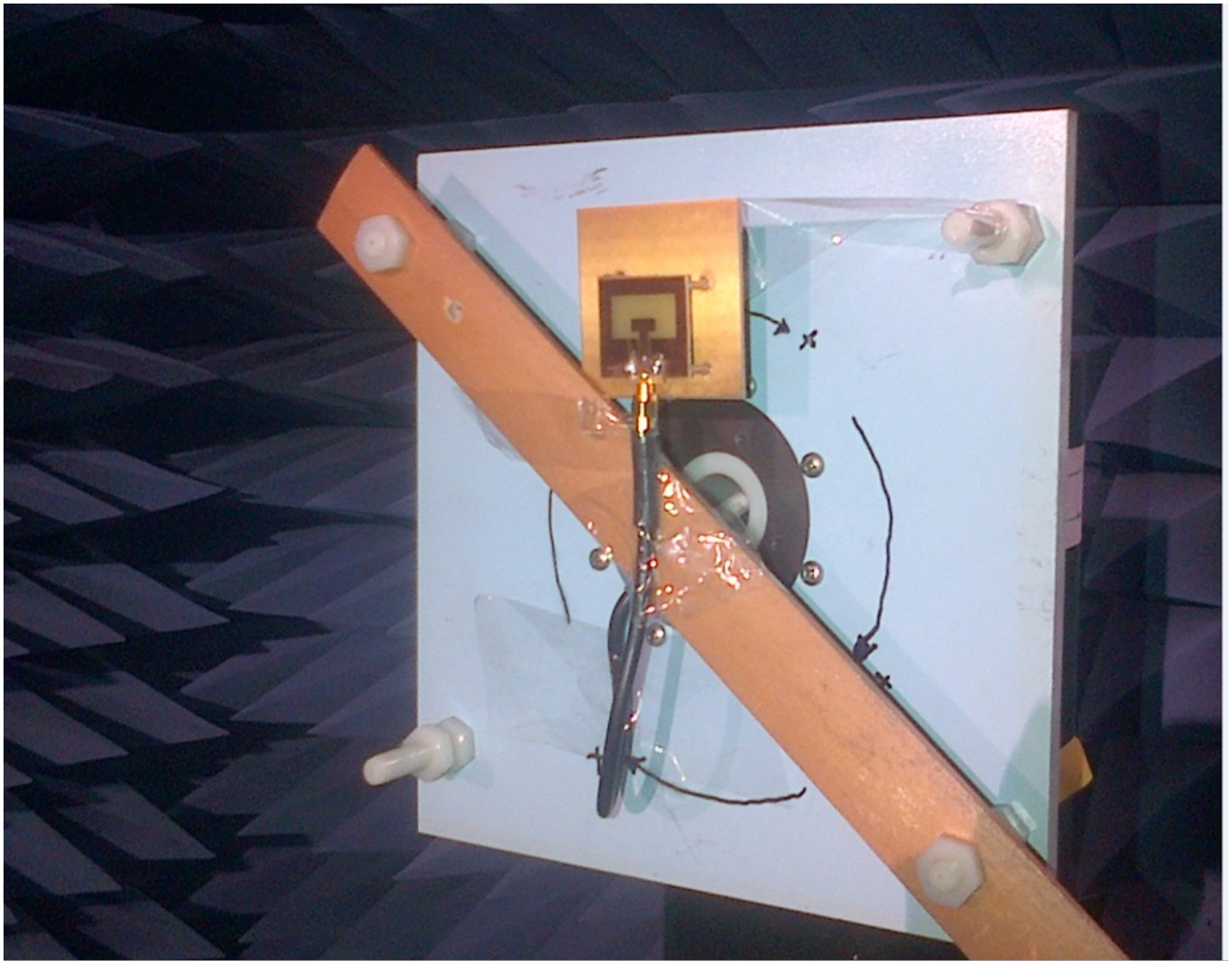
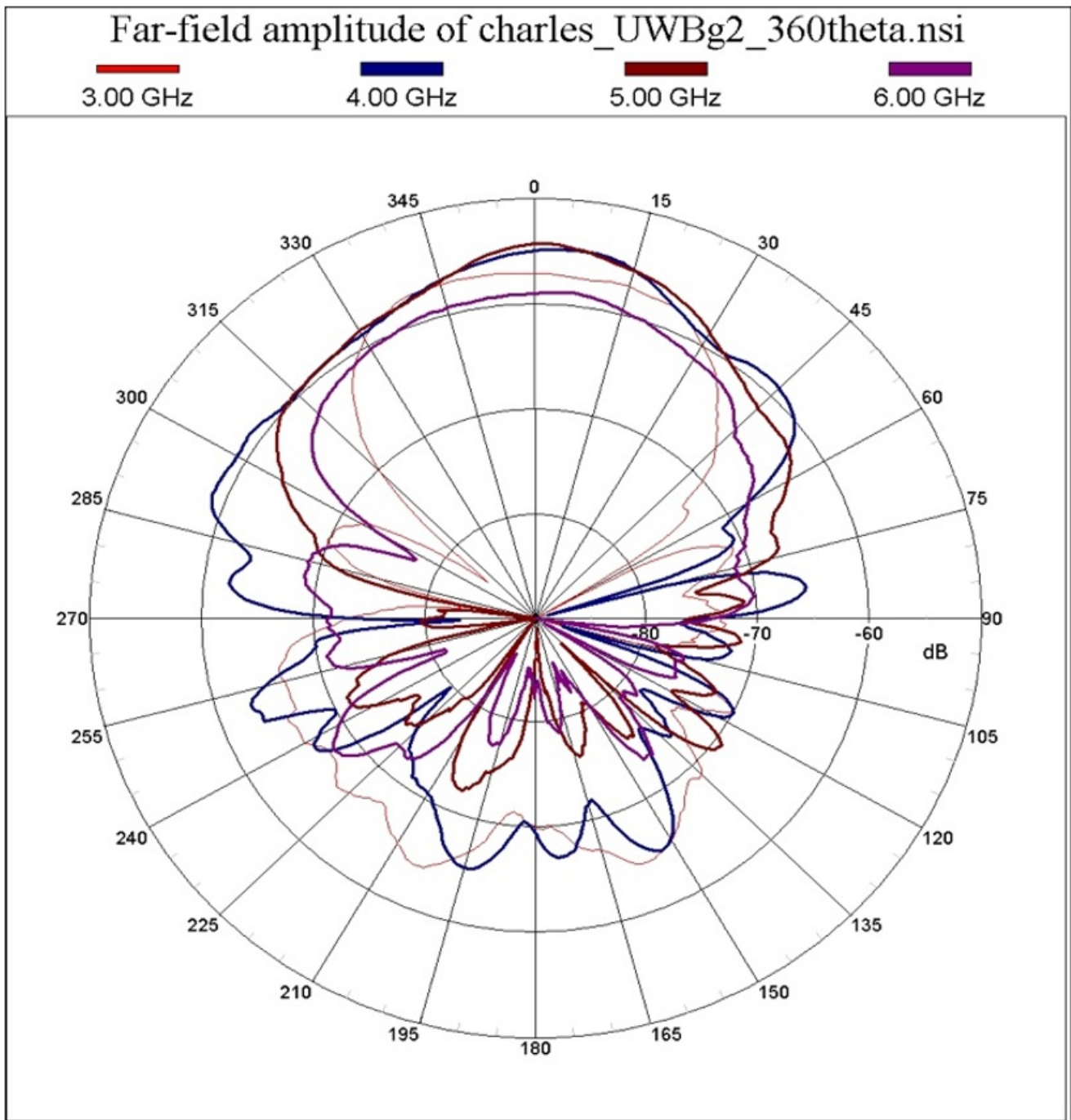


Fig. 24. Return Loss of the Simulated Result with Comparison with the Measured Result (Source- The Author)

The radiation pattern of the proposed antenna with reflector, as measured in the far-field anechoic chamber, is shown in Figure 25.



**Fig. 25.** Measurement Set-Up of the Proposed Antenna with Reflector in the Anechoic Chamber (Source- The Author).



**Fig. 26.** The Measured Far-Field Amplitude Radiation Pattern of the Proposed Antenna (Source- The Author).

The antenna demonstrates good impedance bandwidth ( $S_{11} \leq -10\text{dB}$ ) from about 4GHz to 10.6GHz, except in the case of when the width  $w$  of the T-shaped stub was varied. The proposed antenna achieved good directivity.

#### Investigations on How to Improve the Directivity of the Proposed Antenna

The effect of the size of the reflector on the antenna performance is investigated to see if a better radiation pattern would be achieved compared to the result obtained. The investigation is made by increasing the size of the antenna's reflector by 30% and 50%. The results are analysed in the following subsections:

### Effect of Increasing the Size of the Reflector by 30%

The initial dimension of the reflector is  $60 \times 60 \text{ mm}^2$ ; now the new dimension of the reflector is  $78 \times 78 \text{ mm}^2$  as it is increased by 30%. Simulations are done at 3.1GHz and 4GHz to see the effect of the size of the reflector on the radiation pattern using the CST Microwave Studio. Figures 27 and 28 show the far-field directivity at 3.1GHz and 4GHz, respectively. From the results obtained from the investigation, it can be deduced that a bi-directional radiation pattern is obtained at the two frequencies at which the investigation was carried out.

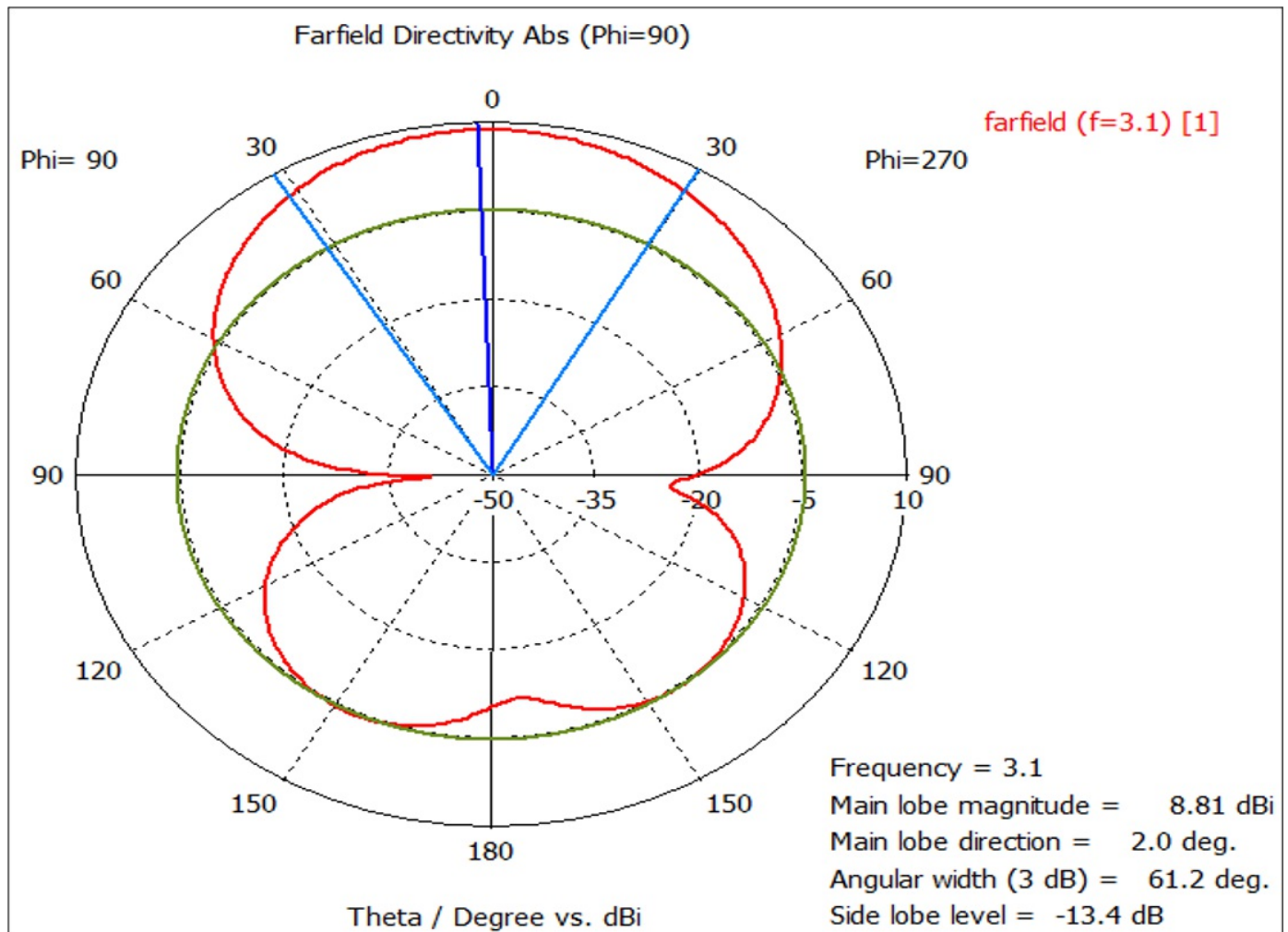


Fig. 27. Far-field Directivity at 3.1GHz of the Proposed Antenna with Reflector Increased by 30% (Source: The Authors)



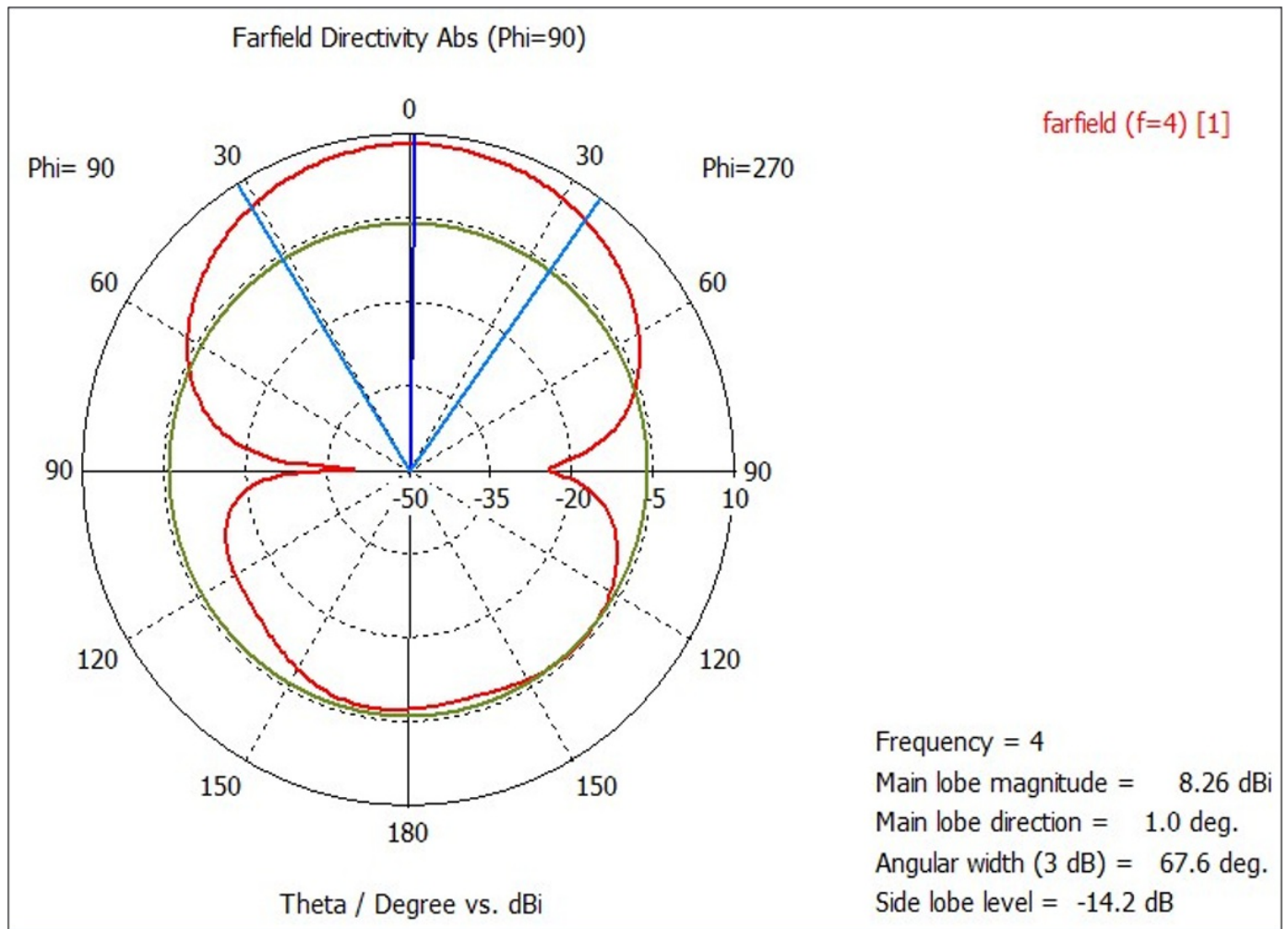


Fig. 28. Far-field Directivity at 4GHz in Polar Plot of the Proposed Antenna with Reflector Increased by 30% (Source: The Authors)

#### Effect of Increasing the Size of the Reflector by 50%

The initial dimension of the reflector is  $60 \times 60 \text{ mm}^2$ ; now the new dimension of the reflector is  $90 \times 90 \text{ mm}^2$  as it is increased by 50%. Simulations are done at 3.1GHz and 4GHz to see the effect of the size of the reflector on the radiation pattern using the CST Microwave Studio. Figures 29 and 30 show the far-field directivity at 3.1GHz and 4GHz, respectively. From the results obtained from the investigation, it can be deduced that a bi-directional radiation pattern is obtained at the two frequencies at which the investigation was carried out.

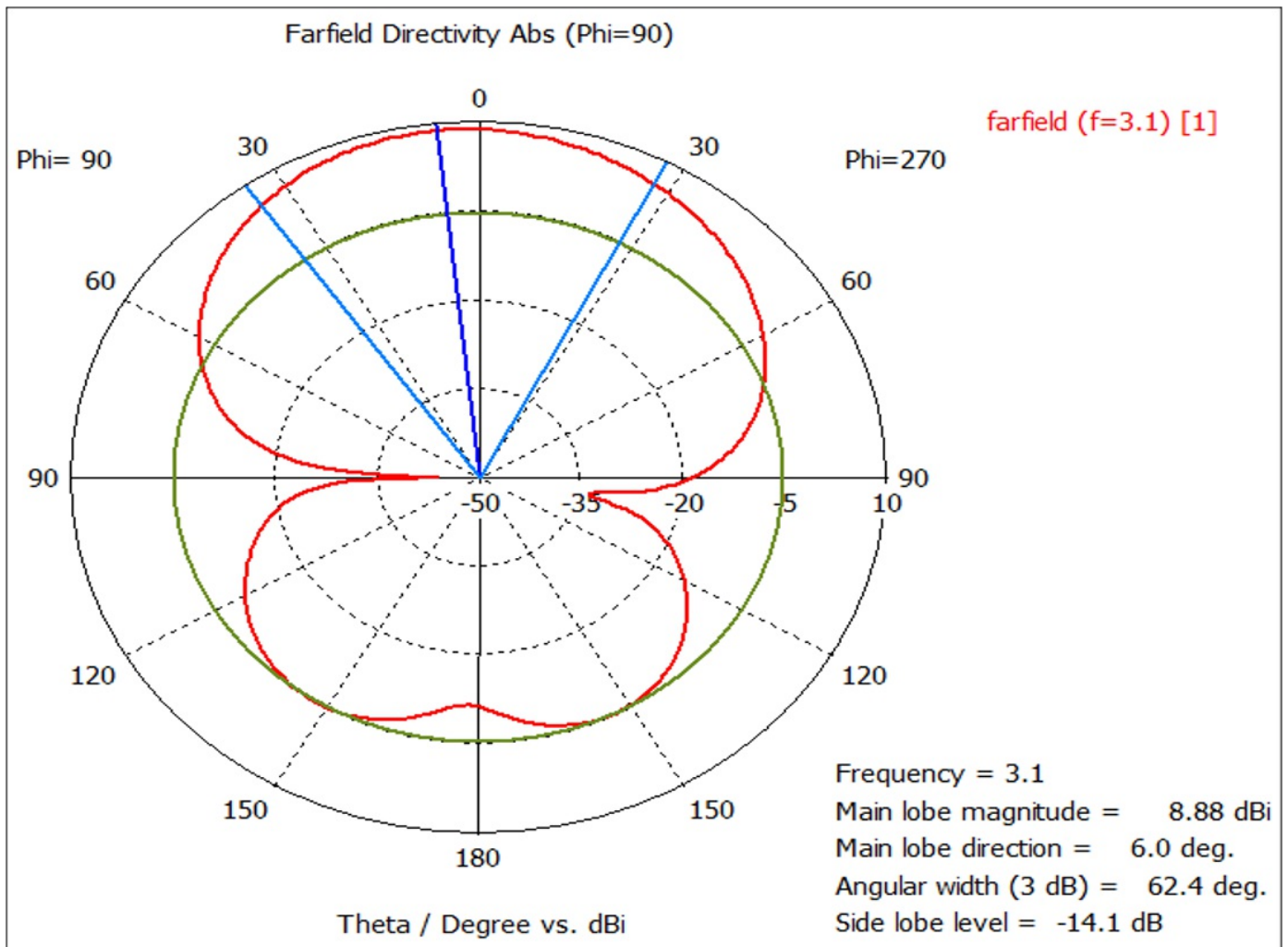


Fig. 29. Far-field Directivity at 3.1GHz of the Proposed Antenna with Reflector Increased by 50% (Source: The Authors)

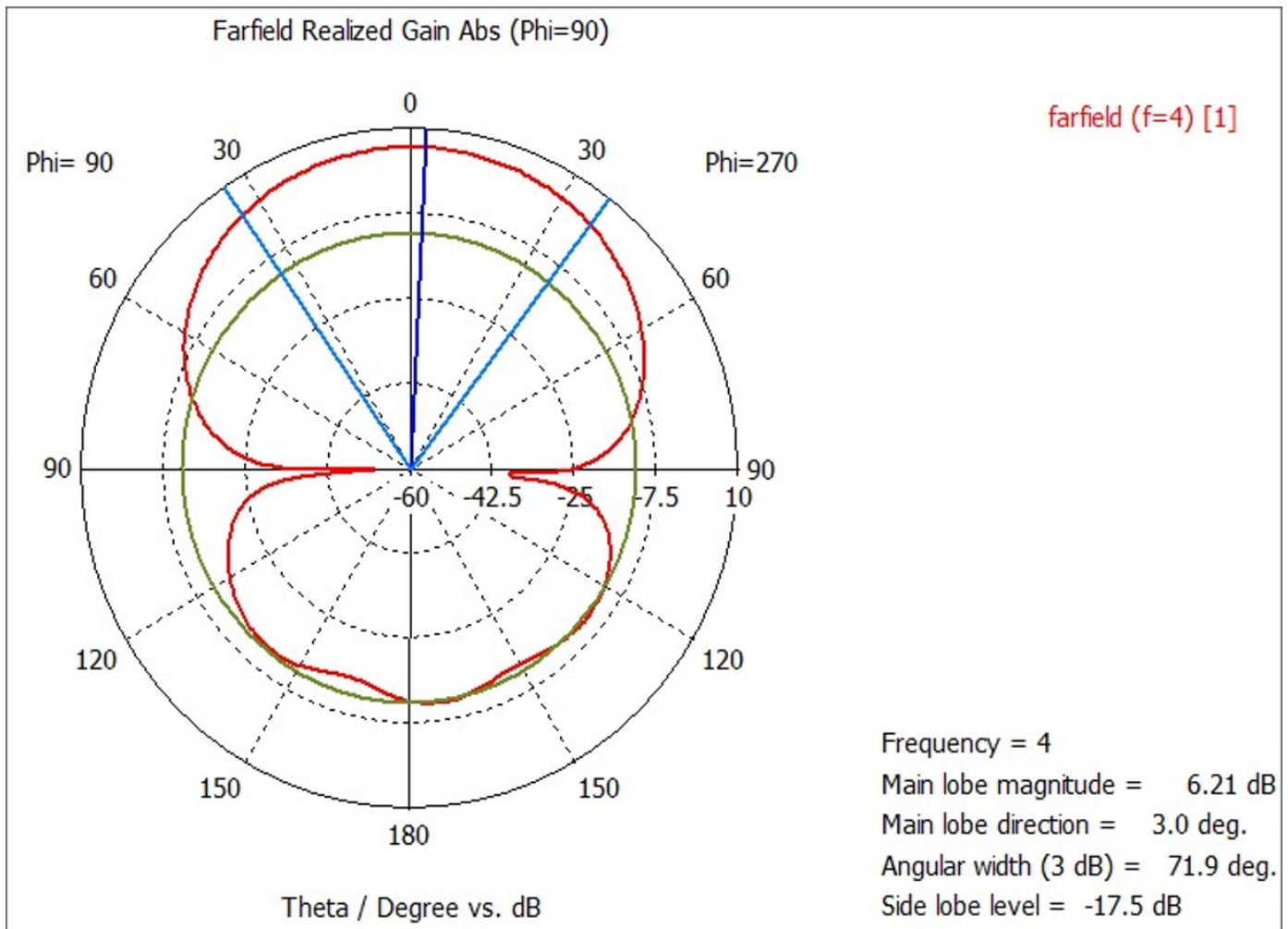


Fig. 30. Far-field Directivity at 4GHz of the Proposed Antenna with Reflector increased by 50% (Source - The Authors)

## 5. Conclusion

In this study, we conclude that the investigations carried out on the radiation pattern of the proposed antenna at the frequencies at which the radiation pattern seems omni-directional from the measured results confirmed that the proposed antenna is not directional at the two frequencies, that is, 3.1GHz and 4GHz, but bi-directional when the size of the reflector was increased by 30% and 50%. An overall better performance of the system is obtained, as seen from the results obtained from the investigations on the proposed antenna with the reflector as carried out in this study. The reflection coefficients ( $S_{11}$ ) as a function of frequency for the proposed antenna with a reflector are illustrated in Figures 12 – 14. The antenna demonstrates good impedance bandwidth ( $S_{11} \leq -10\text{dB}$ ) from about 4GHz to 10.6GHz, except in the case of when the width  $w$  of the T-shaped stub was varied. The radiation patterns of the antenna were analysed and compared. A good directivity was achieved by the proposed antenna. Investigations were further carried out on how the directivity of the designed antenna can be improved at frequencies of 3GHz and 4GHz. This investigation was done by examining the effect of the size of the additional ground plane, known as the reflector, on the radiation pattern of the antenna using the simulation tool CST Microwave Studio.

## Acknowledgments

We acknowledge all articles being referenced during the course of this study, and almighty God for the successful completion of this study.

## Other References

- Sze, J. Y. & Wong, K. L., (2001) "Bandwidth Enhancement of a Microstrip line-feed printed wide-slot Antenna," IEEE Trans. Antennas and Propagation, 49(7), pp. 1020 – 1024. doi: 10.1109/8.933480
- Federal Communications Commission (FCC), 2002. First Report and Order 02 - 48, s.l.: s.n.
- Elsherbini, A. & Sarabandi, K., (2009) "Directive Coupled Sectorial Loops Antenna for Ultra-wideband Applications," IEEE Antennas Wireless Propagation Letters, Volume 8, pp. 576 - 579. doi: 10.1109/LAWP.2009.2020444.
- Allen, B. et al., (2007) "Ultra-wideband Antenna and Propagation for Communications, Radar and Imaging," In: New Jersey: Wiley Press, pp. 134 – 135. DOI:10.1002/0470056843
- Abbosh, A. M., Blalkowski, M. E., Mazierska, J. & Jacob, M. V., (2006) "A Planar UWB Antenna with Signal Rejection Capability in the 4-6GHz band," IEEE Microwave and Wireless Components Letter, 16(5), pp. 278 - 280. doi: 10.1109/LMWC.2006.873500
- Kumar O. et al., (2021) "Ultrawideband Antennas: Growth and Evolution" Micromachines (Basels), 13(1): 60. doi: 10.3390/mi13010060.
- Chen, Z.N., (2007) "UWB antennas: Design and application," In 2007 IEEE 6th International Conference on Information, Communications & Signal Processing (pp. 1-5).
- Mahesh S, Khairnar A. & Hasan M. (2022), "A New Approach to Fractal Antenna Design for UWB Applications: An Analysis" Mathematical Statistician and Engineering Applications. 71(4), pp 332-347.
- Uvarov, A.V., Gerasimov, M.Y. & Uvarov, A.V (2019), "On the Fundamental Limitations of Ultra-Wideband Antennas. J. Commun. Technol. Electron. 64, 229–233. <https://doi.org/10.1134/S1064226919030185>
- Rajkumar, S., Selvan, K. T., & Rao, P. H. (2018), "Compact 4 element Sierpinski K nopp fractal UWB MIMO antenna with dual-band notch. Microwave and Optical Technology Letters, 60(4), 1023–1030. <https://doi.org/10.1002/mop.31092>
- Liu X. L., Wang Z. D., Yin Y. Z., Ren J., and Wu J. J. (2014), "A compact ultrawideband MIMO antenna using QSCA for high isolation," IEEE Antennas Wireless Propag. Lett., vol. 13, pp. 1497–1500.
- Kumar, P.; Ali, T.; Pai, M.M. (2022), "A compact highly isolated two-and four-port ultrawideband Multiple Input and Multiple Output antenna with Wireless LAN and X-band notch characteristics based on Defected Ground Structure," Int. J. Commun. Syst, 35, e5331. <https://doi.org/10.1002/dac.5331>
- Galvan-Tejada, G.M.; Peyrot-Solis, M.A.; Jardón Aguilar, H (2019), "Ultra-Wideband Antennas," Design, Methodologies, and Performance; CRC Press: Boca Raton, FL, USA. <https://doi.org/10.1201/b18624>

## References

1. <sup>a, b, c</sup>Immooev I. Y., (2010) "Practical Applications of UWB Technology," *IEEE Aerospace and Electronic Systems Magazine*, 25(2), pp.36-42. <https://doi.org/10.1109/MAES.2010.5442175>
2. <sup>^</sup>Withington, P. & Fullerton, L (1992) "An Impulse Radio Communications System," *Proceedings on Short-pulse Electromagnetics International Conference on Ultra-wideband*, pp. 113 - 120.
3. <sup>^</sup>Zhenzhen Y., Madhukumar A. S, Francois C (2004) "Power Spectral Density and In-Band Interference Power," *IEEE Communications Society*, Volume 6, p. 3561.
4. <sup>^</sup>Ullah S., Ali M., Hussain A., Kwak K. S. (2010) "Applications of UWB Technology," *The 5th annual International New Exploratory Technologies Conference*, pp. 225 - 232. <https://doi.org/10.48550/arXiv.0911.1681>
5. <sup>a, b</sup>Jafari H. M., Liu W., Hranilovic S., Deen M. J., (2006) "Ultra-wideband Radar Imaging System for Bio-medical Applications," *Journal of Vacuum Science and Technology*, 24(3), pp. 752 – 757. <https://doi.org/10.1116/1.2194028>
6. <sup>a, b</sup>Hagness S. C., Taflove A., Bridges J. E., (1999) "Three-Dimensional FDTD Analysis of a Pulsed Microwave Confocal System for Breast Cancer Detection: Design of an Antenna-Array Element," *IEEE Transactions on Antennas and Propagation*, 47(5), pp. 783–791. <https://doi.org/10.1109/8.774131>
7. <sup>a, b</sup>Surowiec A. J., Stuchly S. S., Barr J. R., Swarup A. (1988) "Dielectric Properties of Breast Carcinoma and Surrounding Tissues," *IEEE Transaction Biomedical Engineering*, 35(4), pp. 257 – 263. <https://doi.org/10.1109/10.1374>
8. <sup>a, b</sup>Qing X., Chen Z. N., (2009) "Compact Coplanar Waveguide fed Ultra-wideband Monopole-like Slot Antenna," *IET Microwaves, Antennas and Propagation*, 3(5), pp. 889–898. <https://doi.org/10.1049/iet-map.2008.0075>
9. <sup>a, b, c, d, e, f, g, h, i, j, k</sup>Qing X., Chen Z. N., (2011) "A Miniaturized Directional UWB Antenna," *IEEE International Symposium on Antennas and Propagation*, pp. 1470-1473. <https://doi.org/10.1109/APS.2011.5996572>
10. <sup>a, b, c</sup>Adesoba, O. C. (2023) "Directional UWB antenna for breast cancer detection," *ITEGAM-JETIA*, 9(41), pp. 15-31. <https://doi.org/10.5935/jetia.v9i41.860>
11. <sup>^</sup>Zhu, F. et al., 2011. "Low Profile Directional Ultra-wideband Antenna for See Through-Wall Imaging Applications," *Progress in Electromagnetics Research*, Volume 121, pp. 124 - 129. doi:10.2528/PIER11080907
12. <sup>^</sup>Chen Z. N., Ammann M. J., Qing X., Wu X., See T. S, Cai A. (2006) "Planar Antennas," *IEEE Microwave Magazine*, 7(6), pp. 63 – 73. <https://doi.org/10.1109/MW-M.2006.250315>
13. <sup>^</sup>Lin Y., Hung K., (2006) "Compact Ultra-wideband Rectangular Aperture and Band-Notched Designs," *IEEE Transactions on Antennas and Propagation*, 54(11), pp. 3075–3077. <https://doi.org/10.1109/TAP.2006.883982>
14. <sup>^</sup>Qing X., Chen Z. N., Chia M. Y. W., (2005) "UWB Characteristics of Disc-cone Antenna," *IEEE Proceedings on International Workshop of Antenna Technology*, pp. 97–100. <https://doi.org/10.1109/IWAT.2005.1461013>
15. <sup>a, b, c, d, e, f, g, h</sup>Ranga Y., Esselle K. P., Matekovits L., Hay S. G. (2012) "Increasing the Gain of a Semicircular Slot UWB Antenna Using an FSS Reflector," *IEEE conference on Antennas and Propagation in Wireless Communications*, pp. 478-481. <https://doi.org/10.1109/APWC.2012.6324954>